Supplementary material S1 for a research article published in 'Environmental Science and Technology'

Global Carbon Benefits of Material Substitution in Passenger Cars until 2050 and the Impact on the Steel and Aluminum Industries

Roja Modaresi[1,*], Stefan Pauliuk,[1*] Amund N. Løvik,[1] and Daniel B. Müller[1]

[1)] Industrial Ecology Programme and Department of Energy and Process Engineering, Norwegian University of Science and Technology (NTNU), NO-7491 Trondheim, Norway.

Supplementary material S1

Content

[*)] Corresponding authors: roja.modaresi@ntnu.no and Stefan.pauliuk@ntnu.no

S1-1) System definition and model documentation

S1-1.1) System definition

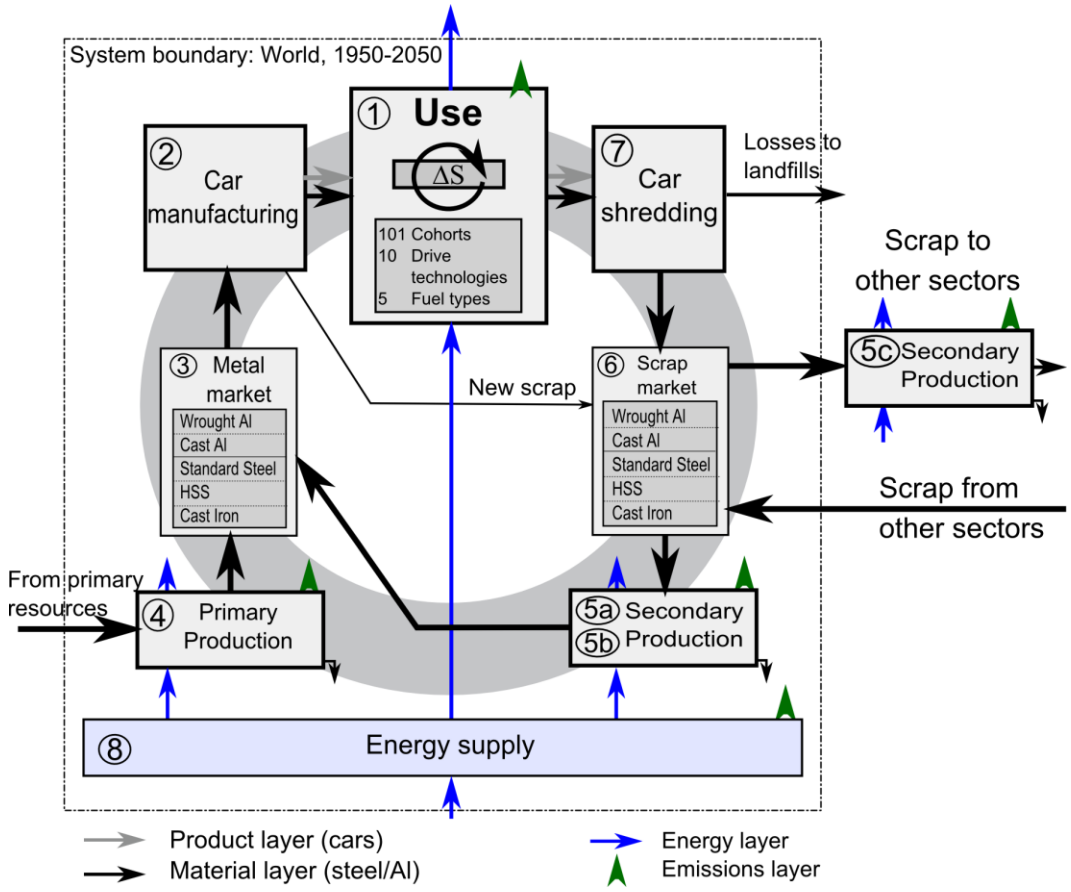

Figure S1-1: System definition. The model time runs from 1950 to 2050. Car flows and stocks are divided into ten drive technologies. Material flows are tracked for cast iron, standard steel, high strength steel, cast aluminum, and wrought aluminum. Six energy carriers are considered: gasoline; diesel; coal; electricity; natural gas; and hydrogen.

Throughout all equations we use the following color code: Grey: Product flows and stocks; Black: Material flows and stocks; Blue: Energy flows; Green: GHG emissions; Brown: Model parameters.

Table S1-1: List of processes and balances.

Process number	Name	Description	Balance
1	Use phase	All passenger vehicles worldwide, 1950-2050, tracked by different cohorts, drive technologies, and fuel types.	Cars, mass, energy
2	Car manufacturing	Models the car industry, characterized by the rate of new scrap generation, or yield loss rate	Mass
3	Metal markets	Maps primary and secondary metal production to manufacturing	Mass
4	Primary metal production		Mass, energy
5a	Secondary production	Uses scrap from other sectors to be recycled into cars	Mass, energy
5b	Secondary production	Uses internal scrap to be recycled into cars	Mass, energy
5c	Secondary production	Uses internal scrap to be recycled and used in other sectors	Mass, energy
6	Scrap market		Mass
7	Car shredding	Determines how much metal is recovered and at which quality	Mass
8	Energy supply	Common supply of different energy carriers	Energy

Table S1-2: List of indices and system variables.

Symbol	Name	Description
Indices (Sets)		
t	Time	Model time (1950-2050)
t'	Cohort	Cohort (1950-2050)
d	Drive technology	1: Conventional Gasoline 2: Gasoline Hybrid 3: Plug-In Hybrid Gasoline 4: Diesel 5: Diesel Hybrid 6: Plug-In Hybrid Diesel 7: CNG/LPG 8: Electricity 9: H_2 Hybrid ICE 10: H_2 Fuel Cell
f	Fuel type	1: Gasoline 2: Diesel 3: Electricity 4: Natural gas 5: Hydrogen 6: Coal
m	Material	1: Wrought Al 2: Cast Al 3: Cast iron 4: Standard automotive steel 5: High strength steel 6: Construction steel, from vehicle scrap

Stocks		
$S_1(t,t',d)$	In-use stock of passenger cars	In-use stock of passenger cars, broken down on cohorts, and drive technologies
$M_1(t,t',d,m)$	In-use stock of materials in passenger cars	In-use stock of materials, broken down on cohorts, and drive technologies, and material type
Flows		
$F_{2-1}(t,d)$	Car production/consumption	
$F_{1-7}(t,t',d)$	Cars scrapped	
$M_{2-1}(t,m)$	Material inflow in new cars	
$M_{1-7}(t,m)$	Material inflow in old cars	
$M_{7-0}(t,m)$	Material lost in landfills	
$M_{7-6}(t,m)$	Material recovered as old scrap	
$M_{2-6}(t,m)$	Fabrication or new scrap	
$M_{3-2}(t,m)$	Material consumption by car industry	
$M_{4-3}(t,m)$	Primary metal production for the car sector	
$M_{0-4}(t,m)$	Input of primary metal resources (metal in ores)	
$M_{5a-3}(t,m)$	Secondary metal production with external scrap for passenger cars	
$M_{0-5a}(t,m)$	Inflow of external scrap from other sectors	E.g., Al scrap from buildings
$M_{5b-3}(t,m)$	Secondary metal production with internal scrap for passenger cars	
$M_{6-5b}(t,m)$	Internal scrap used for recycling back into cars	
$M_{6-5c}(t,m)$	Internal scrap used for recycling and export to other sectors	
$M_{5c-0}(t,m)$	Export of scrap from internal scrap to other sectors	E.g., construction steel
$E_{8-1}(t,f)$	Direct energy consumption by passenger cars	
$E_{8-4}(t,f)$	Direct energy consumption by primary metal production	
$E_{8-5a}(t,f)$, $E_{8-5b}(t,f)$	Direct energy consumption by secondary metal production within the sector	
$E_{0-5c}(t,f)$	Direct energy consumption by secondary metal production from internal scrap outside the sector	
$C_{1-0}(t)$	Direct CO_2 emissions from passenger cars	
$C_{4-0}(t,m)$	Process and direct GHG emissions from primary metal production	
$C_{5a-0}(t,m)$, $C_{5b-0}(t,m)$	Process and direct GHG emissions from secondary metal production	
$C_{8-0}(t)$	Indirect emissions from energy supply ('well-to-tank')	

General comment: A variable of higher aggregation can always be obtained by summing up over certain indices, for example:

$$S_1(t,t') = \sum_d S_1(t,t',d); \quad S_1(t) = \sum_{t'} S_1(t,t'); \qquad \text{(S1)}$$

Below in the text we do not make the summation explicit. When a variable shifts indices from one line to the next, e.g., from *μ(t,t',d,m)* to *μ (t,t',m)*, we implicitly assume that the summation over *d* was carried out in between.

S1-1.2) The model approach

Table S1-3: List of system parameters:

Symbol	Name	Description, section
$P(t)$	Population	
$C(t)$	Car ownership rate	
$\lambda(t-t')$	Lifetime distribution	
$D(t',d)$	Drive technology share	
$\mu(t',d,m)$	Specific material intensity	
$R(t,m,m')$	End-of-life recovery efficiency	
$N(t,m)$	New scrap generation rate	
$SI(t,m)$	Scrap Input per metal output in secondary prod.	
$MMP(t,m)$	*'material match primary'*	Describes the fraction of primary metal in the inflow to car manufacturing
$MMSI(t,m)$	*'material match secondary internal'*	Describes the fraction of secondary metal from internal scrap in the inflow to car manufacturing
$MMSE(t,m)$	*'material match secondary external'*	Describes the fraction of secondary metal from external scrap in the inflow to car manufacturing
WFR	Weight-fuel relationship	Coupling between Energy consumption and mass change. Unit: MJ/(km*kg)
$K(t)$	Annual kilometrage driven	Km/yr
$F(t',d,f)$	Fuel demand specific for each cohort, drive technology, and fuel type	Unit: MJ/km

$e_{prim}(t,m,f)$	Energy intensity of primary metal production, changes over time, is specified for each material and fuel type	Unit: GJ/ton
$e_{sec}(t,m,f)$	Energy intensity of secondary metal production, changes over time, is specified for each material and fuel type	Unit: GJ/ton
$c_{P\_prim}(t,m)$	Process emissions from primary metal production	Unit: tons of CO_2-eq per ton of metal output
$c_{P\_sec}(t,m)$	Process emissions from secondary metal production	Unit: tons of CO_2-eq per ton of metal output
$c_D(t,f)$	Direct emissions intensity	Unit: tons of CO_2-eq per GJ
$c_I(t,f)$	Indirect emissions intensity	Unit: tons of CO_2-eq per GJ

S1-1.2.1) Stocks and flows of passenger cars

The total car stock for each year is given by the product of population and car ownership:

$$S_1(t) = P(t) \cdot C(t) \quad \text{(S2)}$$

The age structure of the stock is determined in a year-by-year calculation, as in previous work [1-3]. For each year, the following calculations are performed: First, the number of cars leaving the use phase is determined for all previous cohorts using the lifetime distribution:

$$\forall t' \le t : F_{1-7}(t,t') = F_{2-1}(t') \cdot \lambda(t-t') \quad \text{(S3)}$$

Then, the total mass balance of the use phase gives the total new inflow:

$$F_{2-1}(t) = \left(S_1(t) - S_1(t-1)\right) + F_{1-7}(t) = \left(S_1(t) - S_1(t-1)\right) + \sum_{t' \le t} F_{2-1}(t') \cdot \lambda(t-t') \quad \text{(S4)}$$

The total consumption of new cars is then split onto different drive technologies, both are assumed to be independent of each other:

$$F_{2-1}(t = t', d) = F_{2-1}(t) \cdot D(t,d)$$
$$F_{1-7}(t,t',d) = F_{1-7}(t,t') \cdot D(t',d) \quad \text{(S5)}$$

The total in-use stock of cars is then broken down into ten drive technologies using the time series for the historic inflows and the lifetime model:

$$S_1(t,t',d) = F_{2-1}(t',d) \cdot \left(1 - \sum_{t' \le t} \cdot \lambda(t-t')\right) \quad \text{(S6)}$$

S1-1.2.2) The material layer

The total material demand for each year is then given by multiplying the inflow with the specific material intensity μ*(t,d,m)*.

$$M_{2-1}(t,m) = \sum_d F_{2-1}(t,d) \cdot \mu(t = t', d, m) \quad \text{(S7)}$$

The material intensity μ allows us to determine the total mass of the metal stock in use as well as the amount of metal leaving the use phase:

$$M_1(t,m) = \sum_{t',d} M_1(t,t',d,m) = \sum_{t',d} F_{2-1}(t',d) \cdot \mu(t',d,m) \cdot \left(1 - \sum_{t''=0}^{t''=t-t'} \lambda(t'')\right) \quad \text{(S8)}$$

$$M_{1-7}(t,m) = \sum_{t',d} F_{2-1}(t',d) \cdot \mu(t',d,m) \cdot \lambda(t-t') \quad \text{(S9)}$$

The available flow of end-of-life material is obtained by multiplying the recovery efficiency of each metal category and mapping the metal to its target category:

$$\begin{aligned} M_{7-6}(t,m') &= \sum_{m} M_{1-7}(t,m) \cdot R(t,m,m') \\ M_{7-0}(t,m) &= M_{1-7}(t,m) \cdot \left(1 - \sum_{m'} R(t,m,m')\right) \end{aligned} \quad \text{(S10)}$$

New scrap generation leads to a higher demand for new material:

$$\begin{aligned} M_{3-2}(t,m) &= \frac{1}{1-N(t,m)} \cdot M_{2-1}(t,m) \\ M_{2-6}(t,m) &= \frac{N(t,m)}{1-N(t,m)} \cdot M_{2-1}(t,m) \end{aligned} \quad \text{(S11)}$$

Losses occur during the recycling process, and we introduce the quantity *SI(t,m)* to denote the amount of scrap needed produce a ton of secondary material of type *m*.

$$SMS(t,m) := M_{5b-3}(t,m) + M_{5c-0}(t,m) = \left(M_{2-6}(t,m) + M_{7-6}(t,m)\right) / SI(t,m) \quad \text{(S12)}$$

Here, S*MS (‘secondary material supply’)* denotes the total available secondary material from scrap from the car sector. Some of the steel scrap is recycling into construction steel (m= 6), which always becomes part of M_{5c-0}. $M_{5b-3}(t,6)$ = 0 for all years *t*.

To match the available internal secondary material, the levels of primary production and exported secondary material to the metal demand from manufacturing, the following quantities are introduced and specified in the next section (S1-1.2.3). *MMP (‘material match primary’)* denotes the fraction of the demand from car manufacturing that is sourced from primary production, MMSI *(‘material match secondary internal’)* the fraction that is sourced from internal scrap and MMSE *(‘material match secondary external’)* the fraction that is sourced from external scrap:

$$\begin{aligned} M_{4-3}(t,m) &= MMP(t,m) \circ M_{3-2}(t,m) \\ M_{5b-3}(t,m) &= MMSI(t,m) \circ M_{3-2}(t,m) \\ M_{5a-3}(t,m) &= MMSE(t,m) \circ M_{3-2}(t,m) \end{aligned} \quad \text{(S13)}$$

The amount of exported secondary material produced from internal scrap is given by the following balance:

$$M_{5c-0}(t,m) = SMS(t,m) - M_{5b-3}(t,m) \quad \text{(S14)}$$

The remaining mass flows $M_{0\text{-}4}$, $M_{0\text{-}5a}$, $M_{6\text{-}5b}$ and $M_{6\text{-}5c}$ are determined by the respective mass balances of the processes 4 and 5a-5c.

S1-1.2.4) The energy layer

We consider energy consumption related to driving the cars and fort the material production within the car sector.

The energy consumption of the use phase is calculated by multiplying the total car stock, broken down into cohorts, and drive technologies, with the annual number of kilometers driven *(K)* and the specific fuel consumption *(F)*, which is specified for each cohort, drive technology, and fuel type:

$$E_{8-1}(t,t',d,f) = K(t) \cdot S_1(t,t',d) \cdot F(t',d,f) \quad \text{(S15)}$$

For the material production industries, we compiled detailed life cycle inventories for the major production processes, assumed efficiency improvements over time, and included process, direct, and indirect emissions. The total energy requirement for the different metal production processes is obtained by multiplying the output mass flows with the specific fuel requirements for each process:

$$\begin{aligned} E_{8-4}(t,m,f) &= e_{prim}(t,m,f) \cdot M_{4-3}(t,m) \\ E_{8-5a}(t,m,f) &= e_{\sec}(t,m,f) \cdot M_{5a-3}(t,m) \\ E_{8-5b}(t,m,f) &= e_{\sec}(t,m,f) \cdot M_{5b-3}(t,m) \\ E_{0-5c}(t,m,f) &= e_{\sec}(t,m,f) \cdot M_{5c-3}(t,m) \end{aligned} \quad \text{(S16)}$$

S1-1.2.5) The emissions layer

There are three sources of carbon emissions in the system. (1) Process emissions, e.g., from burning the anodes in primary Al production. (2) Direct emissions from burning energy carriers on-site, e.g., from burning natural gas for heating up Al scrap in a re-melter. (3) Indirect emissions caused in the energy supply chain. We compiled the process emissions $c_{P\_prim}(t,m)$ and $c_{P\_sec}(t,m)$ as part of the material production process inventories, used fixed numbers for the direct emissions $c_D(t,f)$ (stoichiometrically determined), and compiled a common inventory $c_I(t,f)$ for indirect emissions in the energy supply chain that applies to the use phase of case and the material production processes alike. Then, the resulting carbon flows for process and direct emissions are determined as follows:

$$C_{1-0}(t) = \sum_{t',d,f} E_{8-1}(t,t',d,f) \cdot c_D(t,f)$$

$$C_{4-0}(t,m) = c_{P\_prim}(t,m) \cdot M_{4-3}(t,m) + \sum_{f} E_{8-4}(t,m,f) \cdot c_D(t,f)$$

$$C_{5a/b-0}(t,m) = c_{P\_sec}(t,m) \cdot M_{5a/b-3}(t,m) + \sum_{f} E_{8-5a/b}(t,m,f) \cdot c_D(t,f) \quad \text{(S17)}$$

$$\left(C_{5c-0}(t,m) = c_{P\_sec}(t,m) \cdot M_{5c-0}(t,m) + \sum_{f} E_{0-5c}(t,m,f) \cdot c_D(t,f) \right)$$

The indirect emissions follow from the next equation:

$$C_{8-0}(t) = \sum_{t',d,f} c_I(t,f) \cdot \left(E_{8-1}(t,t',d,f) + E_{8-4}(t,m,f) + E_{8-5a}(t,m,f) + E_{8-5b}(t,m,f) \right) \quad \text{(S18)}$$

$$\left(C_{0-5c-0}(t) = \sum_{f} c_I(t,f) \cdot \left(E_{0-5c}(t,m,f) \right) \right)$$

The indirect emissions can be allocated to the use phase and the metal production processes 4, 5a, and 5b according to the four terms in the equation.

The indirect emissions for supplying energy to process 5c are calculated accordingly, but are not included in the system definition.

Note: Not all energy flows contribute to direct emissions, as they may become part of the product. E.g., the coal in the coking process is only partly burned, the rest leaves the process as coke, and the coal entering the anode baking process in the Al industry leaves the process in form of anodes. These special cases will be dealt with in the section about the inventory.

S1-2) Data gathering and treatment

We now provide the sources, the processing, and the scenario choices (if applicable) for each of the model parameters listed in Table 3.

S1-2.1) Population $P(t)$:

UN population statistics were used for the historic years 1950-2010 and three scenarios were built using the UN population projection for the years 2011-2050 (low, medium and high population).[4]

The values are contained in the data sheet, SI2, **'Use', B7:D107.**

S1-2.2) Cars per capita $C(t)$:

Three scenarios for global car ownership for 1950-2050 were taken from a previous study with the same scope [2] where the historical data is a weighted average calculation based on individual countries [5-7] and projection cars per capita is calculated based on IEA projections[8]. The scenarios for car ownership from ([2]) were scaled with a constant factor, so that the numbers now only include 'light duty vehicles', or passenger cars, and no busses or light trucks. The scaling factor was chosen so that in 2007, the world population multiplied with the car ownership rate gives a vehicle fleet size of 780 million passenger cars, as reported by the IEA.[8]

The values are contained in the data sheet, SI2, **'Use', E7:G107.**

S1-2.3) Lifetime distribution $\lambda(t-t')$:

Our vehicle lifetime data and assumptions were based on previous studies on car lifetime from the US, and Japan.[9, 10] We assumed vehicle lifetime to follow a normal distribution function with a mean value of 14, 16, and 18 years, and a standard deviation that was 30% of the mean (4.2, 4.8, and 5.4 years), for the low, medium, and high scenarios, respectively.[2]

The values are contained in the data sheet, SI2, **'Use', H7:J107.**

S1-2.4) Drive technology share $D(t',d)$:

Ten drive technologies from IEA's Energy Technology Perspectives were distinguished: [8] Conventional Gasoline: 1, Gasoline Hybrid: 2, Plug-In Hybrid Gasoline: 3, Diesel: 4, Diesel Hybrid: 5, Plug-In Hybrid Diesel: 6, CNG/LPG: 7, Electric vehicles: 8, H_2 Hybrid ICE: 9, H_2 Fuel Cell: 10.

We used the BAU or the BLUE MAP scenario from the IEA for the market shares of the different drive technologies (figure S1-2).[8] Gasoline with 78% and diesel with 19% of market share were the dominating drive technologies in 2005.[8] For the Blue Map scenario the market shares are 14% Gasoline, and Hybrid Gasoline, 25% Plug-in hybrid gasoline, 2% Diesel + Hybrid diesel, 8% Plug-in hybrid diesel, 26% Electric, 5% Natural gas, and 19%

Hydrogen in 2050.[8] The IEA scenarios report results for time intervals of five years, and we performed a linear interpolation to obtain values for the years in between.
The values are contained in the data sheet, SI2, **'Use', AP7:BI107.**

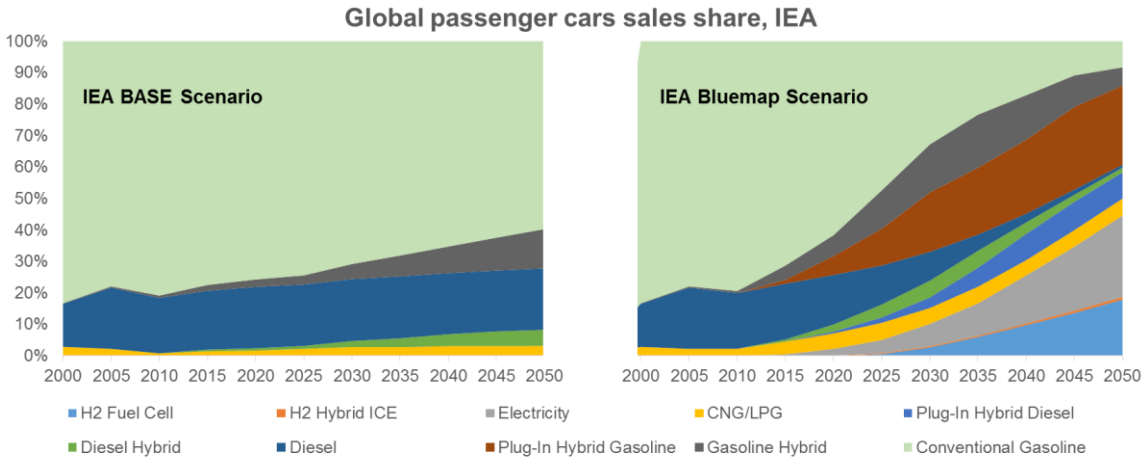

Figure S1-2: Global share of different drive technology for IEA BAU and Blue Map scenario.

S1-2.5) Specific vehicle mass $\mu(t', d, m)$:

The determination of the specific vehicle mass (mass per vehicle) for the baseline and the different light-weighting scenarios was based on a detailed assessment of the light-weighting potential of the different components of a car and a large number of literature sources.
The presentation is split into four parts: a) the current average vehicle material composition and the historic development of the specific vehicle mass (S1-2.5.1), b) the baseline scenario for the specific vehicle mass (S1-2.5.2), c) the description of the DUCKER-light-weighting scenario (S1-2.5.3), and d) the description of our own light-weighting scenarios (S1-2.5.4).

S1-2.5.1) Specific vehicle mass: current average vehicle material composition and historic development

In this procedure, the average passenger car was characterized by considering four component groups: i) Body and closures, ii) Chassis and suspension, iii) Powertrain, iv) Interior and misc. Table S1-4 gives examples of components included in the four groups.

Table S1-4: Component groups and example components.

Component group	***Examples***
Body and closures	Passenger compartment frame, cross and side beams, roof structure, front-end structure, underbody floor structure, panels, doors, hoods, decklids, bumpers
Chassis and suspension	Chassis, suspension, sub-frames, wheels, steering components, brakes, control arms, pedals
Powertrain	Engine, transmission, driveline, exhaust system
Interior and misc.	Seats, instrument panels, trim, electrical components, lighting

For each of these groups, an estimate was made of the material composition by 6 material groups: i) Flat rolled mild steel and ferrous material not elsewhere classified (hereafter referred to as *standard steel*) ii) Flat rolled medium, high and advanced high strength steel (hereafter referred to as HSS) iii) cast iron iv) wrought aluminium, v) cast aluminium, vi) others (e.g. copper, glass, plastics, textiles). A number of different sources were used to arrive at the final estimate, since there is no published literature which uses both component-level and material-level resolution. Table S1-5 gives an overview of the estimation procedure of material content in each component group, where the letter indicates data source and method:

Table S1-5: Characterization procedure overview.

	Standard steel	**HSS**	**Cast iron**	**Wrought Al**	**Cast Al**	**Others**	**Total**
Body and closures	J	E	F	B	B	H	D
Chassis and suspension	J	G	I	B	B	H	D
Powertrain	K	F	I	B	B	L	D
Interior and misc.	K	F	F	B	B	L	D
Total	A	A	A	B	B	A	C

A – Taken directly from Ducker Worldwide. [11]
B – Taken directly from EAA and Ducker Worldwide. [12]
C – Calculated by mass balance of all material contents.
D – Estimated from the distribution of weight in percentage between the component groups as indicated by Lutsey.[13]
E – Taken from America Iron and Steel Institute, for an average unibody construction (the type of body used for almost all non-pickup light vehicles).[14]
F – Assumed equal to zero. Note that certain high-strength steel components which are not flat rolled are included in the *Standard steel* because data sources do not distinguish between mild steel and high strength steel for components that are not flat rolled.
G – Mass balance of all HSS.
H – Taken from Hawkins *et al*.[15]
I – Cast iron distributed as 84% in powertrain and 16% in chassis and suspension, based on Hawkins *et al*. [15]
J – Calculated by mass balance of *total body and closures* and *chassis and suspension* weight.
K – Rest of standard steel split by 62% in powertrain and 38% in interior and misc., based on America Iron and Steel Institute.[14]
L – Calculated by mass balance of total *powertrain* and *interior and misc.* component group weights.

The review resulted in the following estimate of current average material composition.

Table S1-6: Material composition of vehicle component groups. All numbers in kg.

	Standard steel	**HSS**	**Cast iron**	**Wrought Al**	**Cast Al**	**Others**	**Total**
Body and closures	277	227	0	9	0.4	56	**569**
Chassis and suspension	254	52	22	12	29	46	**414**
Powertrain	123	0	117	5	51	134	**431**
Interior and misc.	76	0	0	15	3	216	**311**
Total	**730**	**278**	**139**	**42**	**83**	**452**	**1725**

These numbers reflect an average North American vehicle around 2010, which is larger than the global average. Therefore the mass of each material and component was scaled down by a scalar factor to give a total vehicle mass of 1382 kg in accordance with global average vehicle mass, as shown in Table S1-7.

Table S1-7: Material composition of vehicle component groups after scaling down to global average. Numbers in kg.

	Standard steel	**HSS**	**Cast iron**	**Wrought Al**	**Cast Al**	**Others**	**Total**
Body and closures	222	182	0	8	0.3	45	**456**
Chassis and suspension	203	41	17	10	23	37	**332**
Powertrain	99	0	94	4	41	108	**346**
Interior and misc.	61	0	0	12	2	173	**249**
Total	**585**	**223**	**111**	**34**	**67**	**362**	**1382**

S1-2.5.2) Specific vehicle mass: BAU 2010-2050

The mass of the five materials cast aluminum, wrought aluminum, cast steel, standard steel, and high-strength steel per vehicle was obtained from consulting firms and industry associations.[16-19] Vehicle mass for BAU is 1382 kg.

S1-2.5.3) Specific vehicle mass: The Ducker scenario

Ducker scenario is based on the Ducker study[20] that attempted to determine the most likely material mix for future North American light vehicles through 2025; by taking into account factors such as technology, cost, material availability, and the fuel economy regulations. Table S1-8 is using the ducker material share and tuned it for the global average vehicle weight.

Table S1-8: global average material content and vehicle mass[17]

Material category	**2010**	**2012**	**2015**	**2025**
Standard steel	581	535	452	349
HSS/AHSS	240	260	282	226
Cast iron	112	108	107	99
Wrought Aluminium	33	40	46	57
Cast aluminium	76	83	87	91
All other material	340	370	385	443
Total weight	1382	1396	1359	1265

S1-2.5.4) Specific vehicle mass: Light-weighting scenarios LWE-Steel-intensive, LWE-Al-intensive, and LWE-Al-extreme

The light-weighting scenarios LWE-Steel-intensive, LWE-Al-intensive, and LWE-Al-extreme were developed by looking at the distribution of the materials between different component groups in the vehicles, and using component-specific substitution factors and assumptions about the extent of substitution in each component group by 2030. The component-level resolution does not enter the model calculations, but was used in an intermediate step to arrive at the new material compositions and vehicle mass that were used in the scenarios.

S1-2.5.4.1) Substitution factors steel

A review was performed of component-specific material substitutions of mild steel with MSS, HSS and AHSS to find the typical weight reduction potential. The information sources are mainly technical papers published by the Society of Automotive Engineers (SAE technical papers). Table S1-9 gives examples of steel grades considered mild steel, MSS/HSS and AHSS in this review.

Table S1-9: Steel grades.

Steel category	***Example***
Mild steel	Drawing steel, deep-drawing steel
Medium/high-strength steel	High strength low alloy steel (HSLA) 260-380 MPa (yield strength) Bake hardened (BH) steels Interstitial free (IF) steels
Advanced high strength steel	HSLA 420-550 MPa Dual phase (DP) steels Complex phase (CP) steels Transformation induced plasticity (TRIP) steels Martensitic steels (MS)

All examples involve some kind of redesign of the individual component, or sometimes larger part of a vehicle (e.g the whole BIW), and often new forming methods. Table S1-10 summarizes the result of the literature review.

Table S1-10: Examples of component light-weighting with high-strength and advanced high-strength steel.

Index	Year	Component	Group	Reference material	New material	Mass (kg)	Substitution factor	Notes	Ref.
1	1999	Hood	Body and closures	Mild	HSS	7.74	0.76	Unspecified HSS	[21]
2	1999	B-pillar	Body and closures	Mild steel	HSS	3.7	0.76	Docol 500 YP (microalloyed boron steel)	[22]
3	2001	Door	Body and closures	Mild steel	HSS/AHSS	10.47	0.58-0.78	Stamped outer. Upper range more realistic.	[23]
4	2001	Door	Body and closures	Mild steel	HSS/AHSS	9.77	0.54-0.73	Hydroformed outer. Upper range more realistic.	[23]
5	2002	Body structure	Body and closures	Mild steel	HSS/AHSS		0.75		[24]
6	2002	Hood	Body and closures	Mild steel	HSS/AHSS		0.68		[25]
7	2002	Door	Body and closures	Mild steel	HSS/AHSS		0.73-0.78		[25]
8	2002	Hatch	Body and closures	Mild steel	HSS/AHSS		0.76-0.78		[25]
9	2002	Chassis	Chassis and suspension	Mild steel	HSS/AHSS		0.66		[25]

10	2003	Windshield side pillar	Body and closures	HSS/AHSS, (HSLA280, DP600)	AHSS (DP800, DP1000)		0.83-0.9	Simulation only.	[26]
11	2003	Truck hood	Body and closures	HSS (BH210)	AHSS (DP500)	114	0.77		[27]
12	2008	Transmission cross member	Chassis and suspension	Mild steel	AHSS (DP600)		0.72-0.77		[28]
13	2009	Center pillar structure (SUV)	Body and closures	Mild steel	AHSS (DP980)		0.65		[29]
14	2009	BIW side, roof structure	Body and closures	HSLA	AHSS (DP600-780)		0.93		[30]
15	2011	Front subframe	Chassis and suspension	HSLA	AHSS (MS)		0.65		[31]
16	2011	Longitudinal member	Body and closures	AHSS (DP 600)	AHSS (DP 600)	6.52	0.84	Only redesign	[32]
17	2011	Longitudinal member	Body and closures	AHSS (DP 600)	AHSS (TPN-W 780)	6.57	0.73		[32]
18	2012	Door	Body and closures	Mixed grades of steel	Mixed grades of steel		0.87-0.89	Weight reduction mainly by sandwich plastic in outer panel.	[33]

19	2001	Wheels	Chassis and suspension	Mild steel	HSLA	9.8	0.86		[34]
20		Front suspension	Chassis and suspension		Mixed grades	44.2		No reference component	[35]
21		Rear suspension	Chassis and suspension		Mixed grades	25.8		No reference component	[35]
22		Pedals	Chassis and suspension		Mixed grades	6.7		No reference component	
23		Parking brake	Chassis and suspension		Mixed grades	2.1		No reference component	[35]
24		Wheels	Chassis and suspension		Mixed grades	16.2		No reference component	[35]
25		Steering, incl. power system	Chassis and suspension		Mixed grades	23.2		No reference component	[35]
26		Brake system	Chassis and suspension		Mixed grades	36.9		No reference component	[35]
27	2002	Total chassis (excl. drive shafts)	Chassis and suspension		Mixed grades	182	0.92	Reference component is a typical C-class chassis.	[35]
28	2006	Generic crash-sensitive body components	Body and closures	HSLA	AHSS (DP)		0.8		[36]

29	2011	Control arm	Chassis and suspension	Wrought Al (AA6082)	AHSS (DP)	3.08-3.2	1-1.04		[37]
30	2007	Seat rail	Interior	HSLA	AHSS (multiphase 1300M)		0.8		[38]

S1-2.5.4.2) Substitution factors aluminum

The component-specific weight reduction potential when substituting mild steel, medium/high-strength steel or cast iron with wrought or cast aluminium was estimated by a literature review. The source of information is the Aluminium Automotive Manual by the European Aluminium Association (EAA) which contains numerous examples from specific car models. The results are summarized in Table S1-11.

Table S1-11: Examples of component light-weighting with aluminium.

Index	Year	Component	Group	Reference material	New material	Mass (kg)	Substitution factor	Notes	Ref.
1	1981	BIW	Body and closures	Steel	Wrought Al	161	0.60	Porsche	[39]
2	1989	BIW	Body and closures	Steel	Wrought Al	163	0.45	Honda Acura NSX	[39]
3	1990's	BIW	Body and closures	Steel	Wrought Al, Cast Al	182	0.46	Ford P2000	[39]
4		BIW	Body and closures	Steel	Wrought Al	132	0.60	GM EV1	[39]
5	2003	BIW	Body and closures	Steel	Wrought Al (90%), Cast Al (10%)	295	0.60	Jaguar XJ	[39]
6		BIW	Body and closures	Steel	Wrought Al (80%), Cast	379	0.61	Range Rover L405	[39]

					Al (15%), HSS (4%), Steel (1%)				
7	1994	BIW and closures	Body and closures	Steel	Wrought Al (78%), Cast Al (22%)	249	0.55	Audi A8 (D2)	[39]
8	1999	BIW and closures	Body and closures	Steel	Wrought Al (78%), Cast Al (22%)	153	0.57	Audi A2	[39]
9	2002	BIW and closures	Body and closures	Steel	Wrought Al (66%), Cast Al (34%)	277	0.62	Audi A8 (D3)	[39]
10	1999	BIW	Body and closures	Steel	Wrought Al	275	0.70	BMW Z8	[39]
11	2012	Body structure	Body and closures	Steel	Wrought Al (47%), Cast Al (45%), Steel (8%)	257	0.70	Mercedes-Benz SL (R231)	[39]
12	1998	Engine cradle	Body and closures	Steel	Wrought Al, Cast Al	14.4	0.66	Ford P2000	[40]
13	1999	Engine cradle	Body and closures	Steel	Wrought Al		0.63	General Motors	[40]
14		Front end carrier	Body and	Steel	Cast Al		0.85	Audi	[40]

			closures						
15		Instrument panel support	Body and closures	Steel	Wrought Al		0.60	generic weight reduction potential	[40]
16	1998	Decklid	Body and closures	Steel	Wrought Al	8.6	0.61	Ford P2000	[40]
17		Wings	Body and closures	Steel	Wrought Al		0.48	generic weight reduction potential	[40]
18		Doors	Body and closures	Steel	Wrought Al		0.63	Renault Espace and Vel Satis	[40]
19		Doors	Body and closures	Steel	Wrought Al		0.56	BMW and Novelis	[40]
20		Bumper system	Body and closures	Steel	Wrought Al		0.50-0.70	generic weight reduction potential	[41]
21		Seats	Interior and misc.	Steel	Wrought Al		0.73	generic weight reduction potential	[42]
22	1998	Rear axle subframe	Chassis and suspension	Steel	Cast Al		0.60	Alcoa	[43]
23		Rear axle subframe	Chassis and suspension	Steel	Wrought Al		0.60	BMW 5, Hydro Rolled Products	[43]

24		Front axle subframe	Chassis and suspension	Steel	Cast Al	2.6	0.55	Volkswagen Lupo, Hydro Rolled Products	[43]
25		Shock absorber	Chassis and suspension	Steel	Wrought Al		0.75	Aleris ZFSachs	[44]
26	2006	Control arm	Chassis and suspension	Steel	Wrought Al	1.7	0.50	Mercedes, Constellium	[44]
27	1996	Wheels	Chassis and suspension	Steel	Cast Al		0.70-0.85	Otto-Fuchs Metallwerke	[45]
28	1996	Wheels	Chassis and suspension	Steel	Wrought Al		0.60-0.80	generic weight reduction potential	[45]
29		Engine block	Powertrain	Cast iron	Cast Al		0.45-0.60	generic weight reduction potential	[46]

S1-2.5.4.3) Average substitution factors

Based on the review of material substitution factors for individual components, average substitution factors were calculated. No distinction between HSS and AHSS was used here because the best result will often be achieved with a combination of different steel grades. The resulting component-specific substitution factors are shown in table S1-12.

Table S1-12: Estimated average substitution factors for the four component groups and five substitution options. Note that this table has the same component classes as tables S1-6 and S1-7.

	Steel to HSS/AHSS	**Cast iron to cast Al**	**Steel to cast Al**	**Steel to wrought Al**	**HSS/AHSS to wrought Al**
Body and closures	0.72	N/A	0.85	0.58	0.81 [e]
Chassis and suspension	0.72	0.53 [b]	0.64	0.64	0.89 [e]
Power train	1 [a]	0.53	N/A	0.65 [d]	N/A
Interior and misc.	1 [a]	N/A	0.73 [c]	0.73	N/A

[a] Assumed no significant weight reduction since no examples were found of this substitution. This may reflect the fact that power train components are often already high-strength steel but nevertheless included in standard steel here due to not being flat rolled.

[b] Assumed equal to substitution factor for cast iron to cast aluminium in power train components.

[c] Assumed equal to substitution factor for steel to wrought aluminium in interior and misc. components.

[d] Assumed equal to average of all examples of steel to wrought aluminium substitution.

[e] Calculated from substitution factor of steel to HSS/AHSS and steel to wrought aluminium.

S1-2.5.4.4) Secondary mass savings

Secondary mass savings are further weight reductions in other parts of the vehicle which are enabled after a primary weight saving e.g. by material substitution. This results from the fact that the size of some components is determined by the need for them to carry the weight of others. The first round of secondary savings can enable further mass reductions, and this process can continue until these savings converge to the full *mass decompounding* potential enabled by the primary savings. The secondary savings are very important, as they can lead to a further weight reduction that is about the same magnitude as the primary savings.[47] Therefore, secondary savings were included by following the approach used by Alonso *et al.*[47] For any primary mass reduction, the secondary savings in each component group after one round of iterations is estimated as the primary weight reduction times a component-specific *mass influence coefficient*. After full mass decompounding, the final secondary weight reduction is estimated as the primary weight reduction times a component-specific *mass*

decompounding coefficient. We refer to the paper by Alonso *et al.* for a description of this approach as well as the values for the coefficients.[47]

S1-2.5.4.5) Scenario assumptions

Taking the current composition of vehicles as a starting point, we defined the scenarios by assuming a) how much of the standard steel, HSS, and cast iron in the various components are to be substituted by 2030, and b) what materials they are substituted with. Table S1-13 gives an overview of the assumptions for the three LWE scenarios.

Table S1-13: Substitution rates under different light-weighting scenarios.

Name	***Theme***	***Substitution levels in 2030***
LWE-Steel-intensive	HSS intensive	• 100% of standard steel in body and closures replaced with HSS • 25% of standard steel in chassis and suspension replaced with HSS
LWE-Al-intensive	Aluminum intensive	• 100% of standard steel in body and closures replaced with aluminum (20% cast, 80% wrought) • 25% of standard steel in chassis and suspension replaced with aluminum (70% cast, 30% wrought)
LWE-Al-extreme	Aluminum extreme	• 100% of standard steel in body and closures replaced with aluminum (20% cast, 80% wrought) • 100% of HSS in body and closures replaced with wrought aluminum • 25% of standard steel in chassis and suspension replaced with aluminum (70% cast, 30% wrought) • 100% of cast iron in chassis and suspension replaced with cast aluminum • 50% of cast iron in power train replaced with cast aluminum • 100% of standard steel in interior replaced with wrought aluminum

The following symbols are used to calculate the weight savings:

- $\mu_{m,i}^{2010}$ - Mass of material *m* in component *i* in 2010.
- $\mu_{m,i}^{2030,ps}$ - Mass of material *m* in component *i* in 2030 after primary savings.
- $\mu_{m,i}^{2030,ss}$ - Mass of material *m* in component *i* in 2030 after one round of secondary savings.
- $\mu_{m,i}^{2030,md}$ - Mass of material *m* in component *i* in 2030 after full mass decompounding.
- $h_{m,i}$ - Share of original mass of material *m* in component *i* which is substituted.
- $k_{n,m,i}$ - Share of the substituted material *n* which is replaced with material *m* in component *i*.
- $q_{n,m,i}$ - Substitution factor for replacing material *n* with material *m* in component *i.* A substitution factor of 0.6 means that 0.6 kg of the new material (e.g. wrought aluminum) can replace 1 kg of the old material (e.g. standard steel).
- γ_i - Mass influence coefficient for component *i*.
- Γ_i - Mass decompounding coefficient for component *i*.

From the substitution rates in Table S1-13 and the substitution factors from Table S1-13, the material compositions resulting from primary savings in 2030 were calculated with the following equation, where on the right-hand side the first term includes the original mass and the decrease in mass of material *m* due to removal, and the second term is the new mass of material *m* if it is used to replace other materials.

$$\mu_{m,i}^{2030,ps} = \mu_{m,i}^{2010}\left(1-h_{m,i}\right)+\sum_{n}\mu_{n,i}^{2010}h_{n,i}k_{n,m,i}q_{n,m,i}$$

The compositions after one round of secondary savings were calculated as:

$$\mu_{m,i}^{2030,ss} = \mu_{m,i}^{2030,ps} - \gamma_i \frac{\mu_{m,i}^{2030,ps}}{\sum_{m}\mu_{m,i}^{2030,ps}}\sum_{m}\sum_{i}\left(\mu_{m,i}^{2010}-\mu_{m,i}^{2030,ps}\right)$$

where on the right-hand side the first term is the initial mass of material *m* in component *i* and the second term represents the secondary savings enabled by the sum of all primary savings. The compositions after full mass decompounding were calculated using the same approach, only replacing the mass influence coefficient with the mass decompounding coefficient:

$$\mu_{m,i}^{2030,md} = \mu_{m,i}^{2030,ps} - \Gamma_i \frac{\mu_{m,i}^{2030,ps}}{\sum_{m}\mu_{m,i}^{2030,ps}}\sum_{m}\sum_{i}\left(\mu_{m,i}^{2010}-\mu_{m,i}^{2030,ps}\right)$$

The equations used for secondary savings reflect the approach taken by Alonso *et al.*[47] The composition in 2030 for the three light-weighting scenarios LWE-Steel-intensive, LWE-Al-intensive, and LWE-Al-extreme with three different levels of secondary savings (none, 1 iteration, infinite iterations) are given in the spreadsheet **"Wt red scenarios"** in the supplementary data file S2. Table S1-14 summarizes the weight savings achieved in the light-weighting scenarios with the three different levels of secondary savings.

Table S1-14: Mass savings in 2030 relative to initial composition.

Scenario name	***Primary savings only***	***One round of secondary savings***	***Full mass decompounding (infinite iterations)***
LWE-Steel-intensive	6%	8%	11%
LWE-Al-intensive	7%	11%	14%
LWE-Al-extreme	13%	20%	26%

Because we want to explore the maximum potential for emissions reductions from light-weighting, we used the variation with full mass decompounding in the main results. The component-level resolution is not needed in the final model, as only the aggregated mass of each material is used. The procedure used to estimate the composition in 2030 does not distinguish between different drive technologies, as it is based on average fleet data. We therefore assume the same aluminum and steel composition for the different drive technologies in 2030, although in our historical data there are minor differences between diesel and gasoline vehicles.

The values for 2030 were calculated as explained above, and for every year between 2010 and 2030, linear interpolation was used to define the content of each material in an average vehicle:

$$\mu(t',d,m) = \mu(2010,d,m) - (t'-2010)\frac{\mu(2030,d,m) - \mu(2010,d,m)}{2030-2010}$$

Hence, the average total vehicle mass also decreases linearly between 2010 and 2030. After 2030 we assume a constant material composition and vehicle mass. See excel sheet "**material into use**" in the supplementary material S2 for the full time series.

S1-2.6) End-of-life recovery rate $R(t,m,m')$:

After becoming obsolete, passenger cars are sent to shredders where a large fraction of their metal content is recovered. Shredding a car into small pieces is a rough recovery process, and the recovered material is often contaminated with other metals, such as copper or tin.[48] One will therefore expect that the secondary material made from passenger cars is not suitable for high quality applications, and recent work on the whereabouts of steel and aluminum confirms this.[49] In the future however, more refined recovery processes may be applied to allow for more re-cycling and less cascading. [50] Hence, rather than applying a simple end-of-life recovery rate, our model includes a recovery matrix R that varies over time and that assigns to each incoming sorted material type *m* a new target material type *m'*. For *m'≠ m* we talk about cascading, and for *m' = m* we talk about re-cycling. For all years t, the row total $\sum_{m'} R(t,m,m')$ gives the total fraction of material m recovered for either recycling or cascading, and is equal to the end-of-life recovery rate. For steel we apply the same total end-of-life recovery rates $\sum_{m'} R(2007,m,m')$ as in ([51]). The former report also includes target values for 2050, and we apply the following values base on:[51]

Table S1-15: Total end-of-life recovery efficiency for automotive steel

Time	Values/Source
Pre 2007	As in 2007, assumption
2007	0.85, [51]
2008-2050	Linear increase from 0.85 to 0.95, assumption
2050	0.95, [51]

For automotive aluminum, we base our assumptions on ([52]).

Table S1-16: Total end-of-life recovery efficiency for automotive aluminum

Time	Values/Source
1950	0.22, [52]
1950-2010	Linear increase from 0.22 to 0.85, assumption
2010	0.85, [52]
2010-2050	Linear increase from 0.85 to 0.95, assumption
2050	0.95, [51]. We assume the same target for Al as for steel, in order to make both sectors comparable.

Tables S1-14 and S1-15 contain the total fraction of recovered metal in the waste streams. What remains to be done is to define the split between cascading and recycling. We developed three scenarios for the full split R(t,m,m') (Table S1-17):

Table S1-17: Scenario overview for the recycling matrix R(t,m,m'):

Scenario	Values, source
BAU	m = 1: all recovered wrought Al is cascaded to cast Al (m'=2) [53] m = 2: all recovered cast Al is recycled to cast Al (m'=2) [53] m = 3: all recovered cast steel is cascaded to construction steel (m'=6)[54] m = 4: all recovered standard steel is cascaded to construction steel (m'=6) [54] m = 5: all recovered high-strength steel is cascaded to construction steel (m'=6) [54]
Closed loop 50	For this scenario, we introduce a new factor *RC*, that linearly increases from 0 in 2010 to 0.5 in 2050. For all recovered material of type *m*, a fraction *RC* is now recycled (*m' = m*), and the remaining *1-RC* are cascaded into a different *m'* as in BAU. In 2035, for example, RC = 0.3125 and the total EOL-recovery rate for standard steel is 0.9125. According to the description above, 0.9125*0.3125 = 28.5% of the standard steel in obsolete cars would be recycled into standard steel, 0.9125*(1-0.3125) = 62.73% would be cascaded into construction steel, and 1-0.9125 = 8.75% would be lost to landfills.
Closed loop 100	As closed loop 50, only that in 2050, the factor RC = 1, which means, all recovered scrap (95%) will be re-cycled back into the same material class. This scenario comes closest to the vision of a circular economy.
Primary	Considers primary production only. Used for comparison only. Under the primary scenario, the recovery matrix is BAU, and all recycled material is exported to other sectors.

The values for the recycling matrices are contained in the data sheet, SI2, **'ELV', C4:AF508.**

S1-2.7) New scrap rate $N(t,m)$:

The new scrap rate in car manufacturing, that is the yield loss rate, was assumed to be constant. Table S1-18 provides an overview of the values chosen and their sources:

Table S1-18: Scenario overview for the new scrap rate:

Parameter	Value	Source
m = 1 (wrought Al)	0.18	[52]
m = 1 (cast Al)	0.03	Assumption, castings are near net shape
m = 3 (cast iron)	0.03	Assumption, castings are near net shape
m = 4 (standard steel)	0.27	[54]
m = 5 (high strength steel)	0.27	[54]

S1-2.8) Scrap input per ton of secondary metal $SI(t,m)$:

Cf. section S1-2.13, which contains the documentation of the energy and emissions inventory.

S1-2.9) Match of material demand to primary and secondary production, $MMP(t,m)$, $MMSI(t,m)$, $MMSE(t,m)$:

We needed to decide how to close the loop between material demand and supply of primary and secondary material. There are three options of how to satisfy metal demand: a) primary production (4), b) secondary production with internal scrap (5b), and c) secondary production with external scrap (5a). In addition, excess internal scrap would be recycled and used in other sectors (5c).

The choice depends on which of the four scenarios BAU, closed loop 50, closed loop 100, or Primary is chosen. Here, *SMS* stands for 'secondary material supply', which is the total available secondary material sources from vehicle scrap (both new and old scrap).

a) **For the *Primary*-scenario:** All material demand is satisfied by primary production:

$$\forall t,m: MMP(t,m)=1,\ MMSI(t,m)=0,\ MMSE(t,m)=0$$
$$M_{5c-0}(t,m)=SMS(t,m) \qquad \text{(S19)}$$

b) **For the other scenarios BAU, closed loop 50, and closed loop 100:** All other scenarios follow the same principle: First, all available internal secondary material is used. If the supply of internal secondary material exceeds the demand from car manufacturing, the difference is exported to other sectors.

$$
\begin{aligned}
&\textit{if } SMS(t,m) \geq M_{3-2}(t,m)\\
&\quad M_{5b-3}(t,m) = M_{3-2}(t,m)\\
&\quad M_{5c-0}(t,m) = SMS(t,m) - M_{3-2}(t,m)\\
&\quad M_{4-3}(t,m) = 0\\
&\quad M_{5a-3}(t,m) = 0\\
&\textit{else}\\
&\quad M_{5b-3}(t,m) = SMS(t,m)\\
&\quad M_{5c-0}(t,m) = 0\\
&\quad M_{4-3}(t,m) = \begin{cases} M_{3-2}(t,m) - SMS(t,m), & m = 1,4,5 \\ 0.52 \cdot (M_{3-2}(t,m) - SMS(t,m)), & m = 2 \\ 0.65 \cdot (M_{3-2}(t,m) - SMS(t,m)), & m = 3 \end{cases}\\
&\quad M_{5a-3}(t,m) = \begin{cases} 0, & m = 1,4,5 \\ 0.48 \cdot (M_{3-2}(t,m) - SMS(t,m)), & m = 2 \\ 0.35 \cdot (M_{3-2}(t,m) - SMS(t,m)), & m = 3 \end{cases} \qquad \text{(S20)}\\
&\textit{end}
\end{aligned}
$$

Second, if the available internal secondary material is not sufficient to fulfill demand, the remaining gap is either filled with primary production or with secondary material from other sectors according to the 2008 world average recycled content that we derived from ([53]) for Al and from ([54]) for steel. Equation S23 shows the relationships used, from which the values for *MMP*, *MMSI*, and *MMSE* can be determined.

Table S1-18a shows the results for the recycled content of the average passenger car in the base year 2010. These values were extracted from the model with the help of equation S13. The average recycled content of the average car is the sum of MMSI and MMSE, where the former indicates vehicle scrap as source (including new scrap from vehicle manufacturing), and the latter metal scrap from other end-use sectors.

Table S1-18a: Initial values for *MMP(2010,m), MMSI(2010,m)*, and *MMSE(2010,m)*. The 2010 values apply to all scenarios, as 2010 is the reference year. **Unit: %.**

Parameter / Material type	***MMP(2010,m)***	***MMSI(2010,m)***	***MMSE(2010,m)***
m = 1 (wrought Al)	83	17 (re-melted fabrication scrap)	0
m = 2 (cast Al)	32	38	30
m = 3 (cast iron)	34	3	63
m = 4 (standard steel)	75	25 (re-melted fabrication scrap)	0
m = 5 (high strength steel)	75	25 (re-melted fabrication scrap)	0

The internal scrap source for wrought Al and steel *MMSI* is scrap from vehicle manufacturing only ('home', 'fabrication', or 'new scrap'), because in 2010, virtually all end-of-life scrap from vehicles was down-cycled into castings (for Al) or construction steel (for steel).

S1-2.10) Weight-fuel relation WFR :

Cheah (2010) [55] provides an extensive review of the weight-fuel relation, and for passenger cars she finds the following coupling between the specific fuel consumption in l/100 km and the vehicle mass in kg:

F [l/100km] = 0.004 [mass/kg] + 3.836.

This coupling factor translates to **WFR = 0.001269 MJ/km*kg**. This number, however, proved to be too crude to adjust the fuel efficiency for different drive technologies and light-weighting. We therefore resumed to a more detailed approach of determining the weight-fuel relation with a sophisticated vehicle simulation model. [56] The approach by FKA[56] assumed the 'New European Driving Cycle' (NEDC), distinguished between primary and secondary weight saving and resizing effects (base power train and re-sized power train), and distinguishes between five different drive technologies (gasoline, gasoline hybrid, diesel, diesel hybrid, and fuel cell vehicle). Table S1-19 shows the values obtained from the study[56] that were used in the model. For reasons of convenience, the unit of measurement is the reduction in fuel consumption in percent for a 10 percent reduction of total vehicle weight. A value of 2.6 means thus that on-the-road emissions will decrease by 2.6 % if the total vehicle weight is reduced by 10%.

Table S1-19: Weight-fuel relation by drive technology, for base and resized power train. **Unit: % per 10%** (means the reduction in fuel consumption in percent for a 10 percent reduction of total vehicle weight). Source: [56]

% per 10%	**Base power train**	**re-sized power train**
Conventional Gasoline	2,6	6,8
Gasoline Hybrid	3,9	5,7
Plug-In Hybrid Gasoline	3,9	5,7
Diesel	3,5	7,1
Diesel Hybrid	3,1	4,9
Plug-In Hybrid Diesel	3,1	4,9
CNG/LPG	2,6	6,8
Electricity	3,1	3,1
H_2 Hybrid ICE	3,9	5,7
H_2 Fuel Cell	5,3	4,9

The values in Table S1-19 for the re-sized power train span from 3.1 to 7.1. This corresponds well with Kim and Wallington (2013), who report a range of 3.2 to 7.1 for the weight-fuel relation used in 33 studies.[57]

S1-2.11) Annual kilometrage $K(t)$:

The three scenarios for the annual kilometrage are the same as in Pauliuk et al. (2012)[3], where a detailed comparison of the time series of kilometrage between both developed and

developing countries was conducted (Table S1-20). The actual values used depend on the model calibration. This is explained in section S1-2.20.

Table S1-20: Scenarios for the annual kilometrage K(t)

Name	Value	Source
BAU	15000 km/yr for all years	[3]
High	18000 km/yr for all years	[3]
Low	12000 km/yr for all years	[3]

S1-2.12) Specific fuel consumption $F(t', d, f)$:

Scenario values for average new passenger vehicles for all drive technologies and the years 2000, 2005, 2010, 2015, 2020, 2025, 2030, 2035, 2040, 2045, and 2050 were taken from scenario model behind IEAs Energy Technology perspectives 2010.[8] Both the BAU and the BLUE map scenarios are represented with two separate data sets. A linear interpolation between the given years was carried out for both BAU and BLUE Map values. For the years before 2000, we assumed the same annual improvement as for the years 2000-2005 reported by the IEA, which is actually mostly irrelevant because most of the drive technologies considered by the IEA report did not exist before 2000. For gasoline cars we made a correction by using estimated global average fuel efficiency of 10l/100 km in 1985, [3]and we made a linear interpolation between 1985 and 2000, and used the same increment for the years before 1985.
The values are contained in the data sheet, SI2, **'Use', BM7:CJ107.**

S1-2.13) Specific energy intensity of primary metal production $e_{prim}(t, m, f)$:

Detailed foreground process inventories were compiled for both steel and aluminum production. The inventories distinguish the following process routes:

Steel:

Primary production of finished (cold rolled) **standard steel**, backwards:
Cold rolling → Hot rolling → Continuous casting → Basic oxygen furnace → Blast furnace → Sintering/Coking

Primary production of finished (cold rolled) **high strength steel**, backwards:
Cold rolling → Hot rolling → Continuous casting → Basic oxygen furnace → Blast furnace → Sintering/Coking

Secondary production of finished (cold rolled) **standard steel**, backwards:
Cold rolling → Hot rolling → Continuous casting → Electric arc furnace

Secondary production of finished (cold rolled) **high strength steel**, backwards:
Cold rolling → Hot rolling → Continuous casting → Electric arc furnace

Primary production of cast iron/steel, backwards:
Continuous casting → Basic oxygen furnace → Blast furnace → Sintering/Coking
(Here, continuous casting was used as proxy for the iron/steel dye casting process.)

Secondary production of cast iron/steel, backwards:
Continuous casting → Electric arc furnace
(Here, continuous casting was used as proxy for the iron/steel dye casting process.)

Aluminum:

Extrusion of primary aluminum, backwards:
Extrusion →Primary ingot casting →Electrolysis →Bauxite refining / (Anode production → Coke production) The chain contains an extra loop for internal re-melting of extrusion scrap.

Primary aluminum casting, backwards:
Shape casting →Primary ingot casting →Electrolysis →Bauxite refining / (Anode production → Coke production) The chain contains an extra loop for internal re-melting of extrusion scrap.

Extrusion of secondary aluminum, backwards:
Extrusion →Refine and re-melt.

Casting of secondary aluminum, backwards:
Shape casting →Refine and re-melt.

We compiled a process inventory for each of the processes in the supply chains listed above. The inventory contains information on the link between foreground processes (e.g., the amount of coke required per kg of anode, and the amount of anode needed per kg of liquid aluminum produced), and information on the energy requirements. The energy carriers considered are the same as for the fuel supply of the use of passenger cars (gasoline, diesel, *electricity*, *natural gas*, hydrogen, and *coal*). To determine emissions from fuel and energy supply we use the same coefficients as for the use phase (cf. section S1-2.18); both the use phase and the production phase hence use the same energy supply system, which is important to consider when modeling on the global scale.

Three types of emissions are considered: Direct emissions from fuel combustion by the processes; process emissions, such as emissions of fluorinated hydrocarbons in aluminum electrolysis; and emissions from fuel and energy supply.

The inventory for **steel production** is presented in the data sheet, SI2, **'Energy Layer Steel'**. The values were compiled from various sources, [50, 51, 54, 58, 59] and for each inventory value, the respective source is given in the Excel sheet. Below the inventories, the process chains are modeled. Here, we assume a general improvement of process energy efficiency of all processes involved of about 23 % over the years 2005-2050, estimated by Milford et al..[58] Milford et al. found that best currently available technology (BAT) is about 23% more efficient than the 2005 average steelmaking technology. Assuming that it takes from 2005 to 2050 to converge to the 2005 best available technology, this gives an annual improvement rate of 0.6%. The same rate was applied retrospectively to estimate the historic energy consumption in the years before 2005.
Production of high-strength steel requires more sophisticated rolling, and as a conservative estimate, we assumed that the entire process route is 27% more emissions intensive that the route for standard steel. This assumption is taken from Table 3 in Kim et al..[8 60]

The inventory for **aluminum production** is presented in the data sheet, SI2, **'Energy Layer Al'**. The values were compiled from various sources,[16, 61-63], and for each inventory value, the respective source is given in the Excel sheet. Below the inventories, the process chains are modeled. Here, we assume a general improvement of process energy efficiency of all processes involved of about 23 % over the years 2005-2050, to be comparable with the steel cycle. The same rate was applied retrospectively to estimate the historic energy consumption in the years before 2005.

S1-2.14) Specific energy intensity of secondary metal production $e_{\mathrm{sec}}(t, m, f)$ **:**

See section S1-2.13.

S1-2.15) Process emissions intensity in primary metal production $c_{P\_prim}(t, m)$ **:**

See section S1-2.13.

S1-2.16) Process emissions intensity in secondary metal production $c_{P\_\mathrm{sec}}(t, m)$ **:**

See section S1-2.13.

S1-2.17) Direct emissions intensity of fuel combustion $c_D(t, f)$ **:**

The direct emissions from fuel combustion are given in Table S1-21:

Table S1-21: The direct emissions by fuel type

Name	Value (kg of CO2-eq/MJ)	Source
Gasoline	0.072	[40]
Diesel	0.071	[64]
Electricity	0	No direct emissions.
Natural gas	0.07	[64]
Hydrogen	0	No direct emissions.
Coal	0.11	[64]

S1-2.18) Indirect emissions intensity of fuel supply $c_I(t, f)$:

The carbon intensity of fuel production and supply (well-to-tank) was taken from a compilation of LCA studies[65, 66] and assumed to be constant over time. The BLUE Map scenario also contains information on the carbon intensity of individual energy carriers, which were not available to us, however. For the BLUE Map scenario, we therefore assumed a linear decline of emissions to 50% of the present levels by 2050, which is in line with the 50% emissions reduction target that defines the BLUE Map scenario.
The values are contained in the data sheet, SI2, **'Use', CK7:CV107**.

S1-2.19) Scenario definition

The arrangement of the different parameter choices into scenarios is documented in the scenario definition table in the data file SI2, sheet **'Cross Scenario Analysis'**.

S1-2.20) Model calibration

The model combines data from a large number of independent sources. When these data are put together in the model, one cannot expect the modeled overall emissions to equal reported values, because the underlying system boundaries that were used to determine the different parameters may not always be the same. An example is the definition of passenger vehicles. This can be interpreted as the number of passenger cars or light duty vehicles (product definition), or as the number of vehicles used for transporting passengers (functional definition). The number of vehicles in the latter category would also include busses, 2- or 3-wheelers, and light trucks, and may be considerably higher than the number of passenger vehicles in some countries.

We use the data on the total number of passenger vehicles and their direct emissions reported by Energy Technology Perspectives 2010 as reference.[8] ETP 2010 reports a fleet size of 780 million vehicles for 2007 (page 259 in ETP 2010), and direct carbon emissions of passenger vehicles in 2007 by 2.1 Gt (figure 7.9 on page 267 in ETP 2010). Divided by the average CO_2 emissions intensity of gasoline of 70g/MJ, this corresponds to about 30 EJ of energy in form of fuel. To match model data with these reported values we

a) Scale the total passenger car ownership so that it leads to a fleet of 780 million units in 2007. With a global population of 6.67 billion people for that year, the resulting global average car ownership rate is 117 per 1000 people. The scaled end values for 2050 are 206, 275, and 345 cars per 1000 people for the low, medium, and high scenarios, respectively.
b) The historic kilometrage is adjusted so that for 2007, the model result for total direct energy demand for operating the global passenger vehicle fleet equals 30 EJ. This leads to an average global kilometrage of 14140 km per year for each vehicle, which is about 6% lower than the start value of 15000 km per year. 14140 km/yr are now the new value, and for the years 2010-2030 we assume that the actual kilometrage will linearly change from the start value of 14140 to its end value of 12000, 15000, or 18000 for the low, medium, and high scenario, respectively. After 2030, the annual kilometrage is assumed to be constant.

S1-3) Additional Results

We present the following additional results:

- Time series for the results of the sensitivity analysis (Figures S1-3 and S1-4)
- Sensitivity analysis of cumulative changes in emissions relative to the BAU scenario (Figure S1-5)
- Cumulative material demand and scrap supply for the sensitivity analysis (Figures S1-6 and S1-7)
- Cumulative material demand and scrap supply for the light-weighting scenarios (Figures S1-8 and S1-9)
- Stocks of materials contained in passenger cars in use for the global passenger vehicle fleet, 2010, 2030, and 2050, specified by light-weighting scenario (Figure S1-10).
- Carbon emission flows from use phase, fuel supply, and metal production for the light-weighting scenarios in 2030, and 2050, respectively (Figures S1-11 and S1-12).
- Carbon emission flows from primary and secondary steel and aluminum production for the light-weighting scenarios in 2030, and 2050, respectively (Figures S1-13 and S1-14).
- Annual total carbon emissions for the light weighting scenarios with and without secondary weight savings (Figures S1-15 and S1-16).
- Cumulative emissions from metal production and recycling (Figure S1-17); and cumulative emissions from metal production, recycling, the use phase, and fuel supply (Figure S1-18).

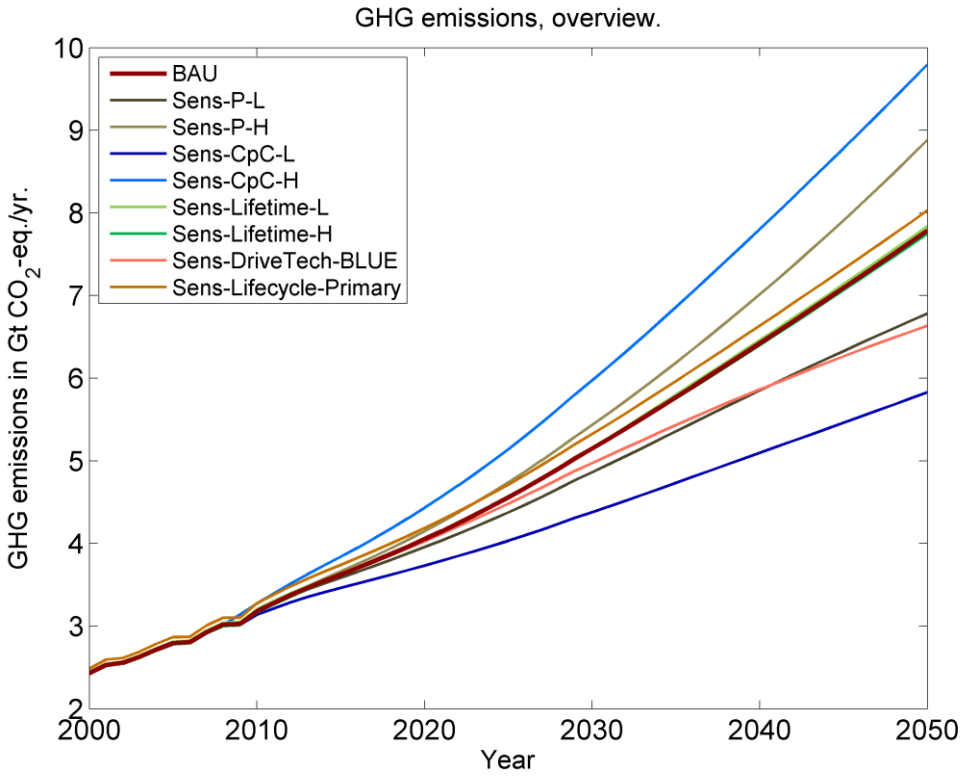

Figure S1-3: Sensitivity analysis, first part.

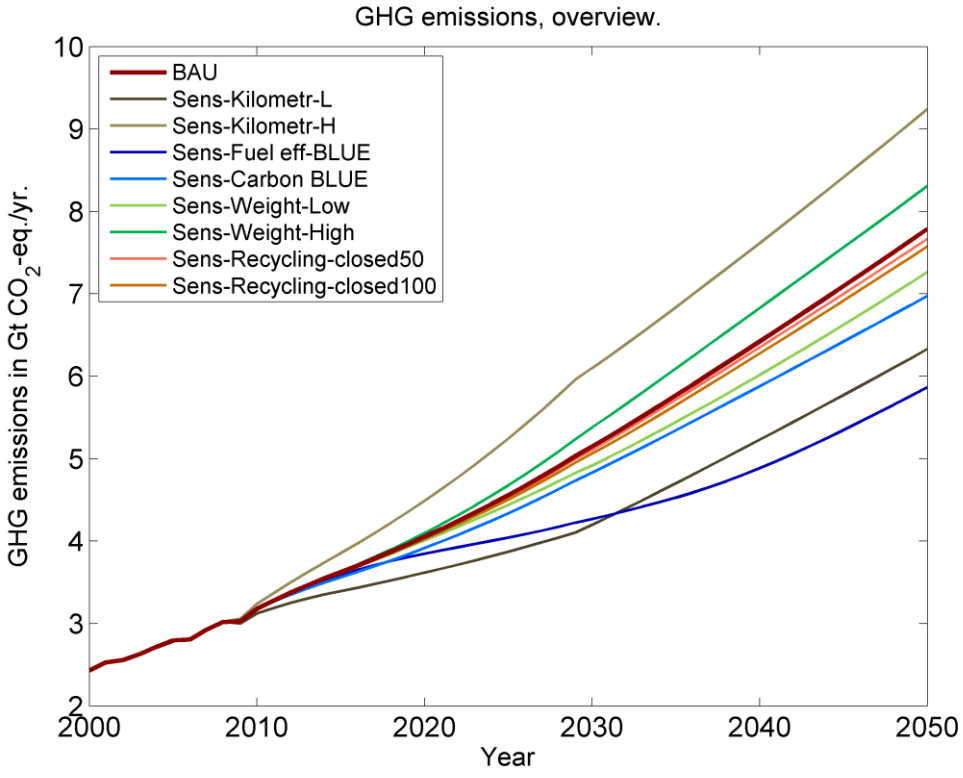

Figure S1-4: Sensitivity analysis, second part.

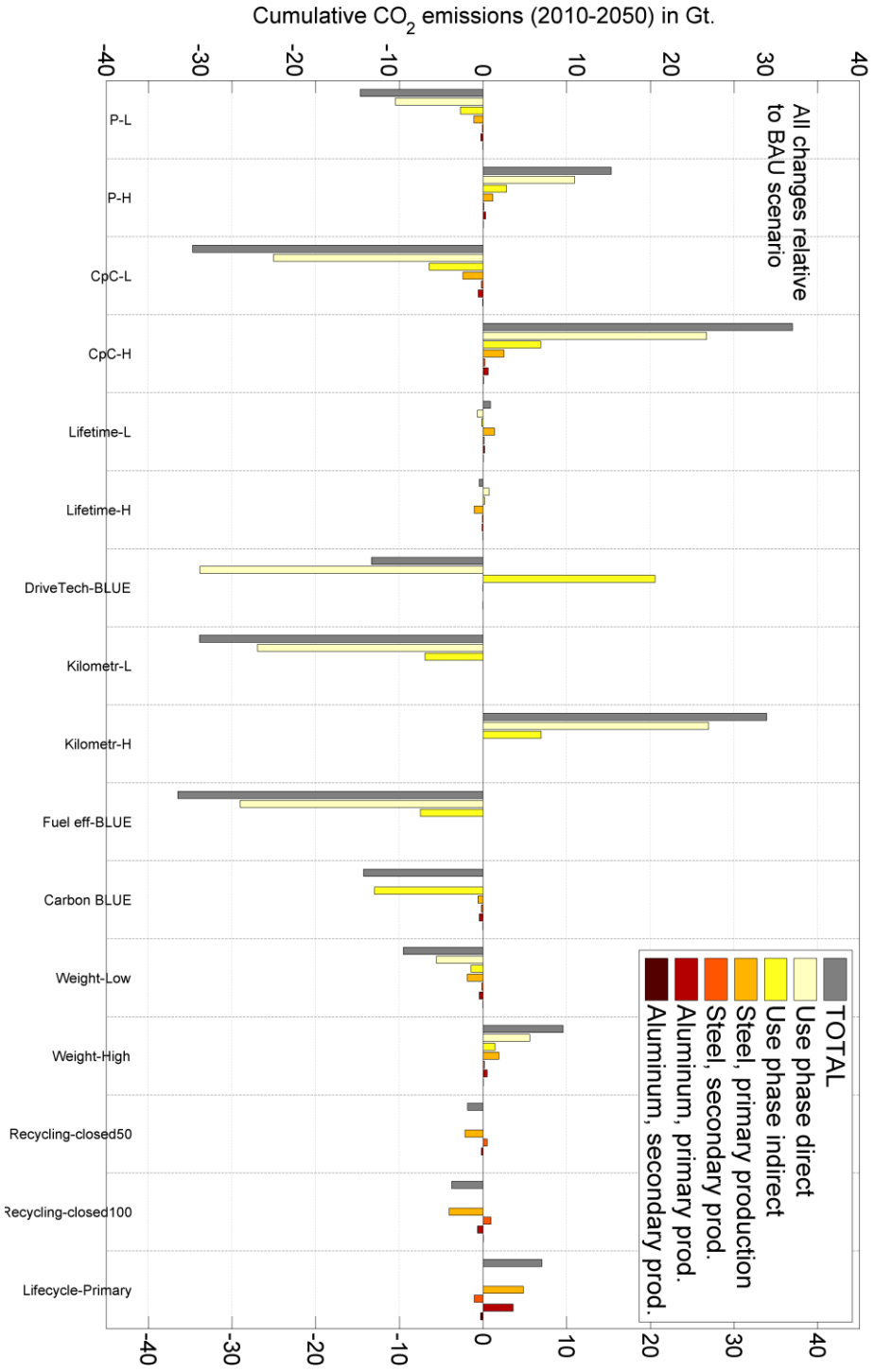

Figure S1-5: Sensitivity analysis, cumulative emissions.

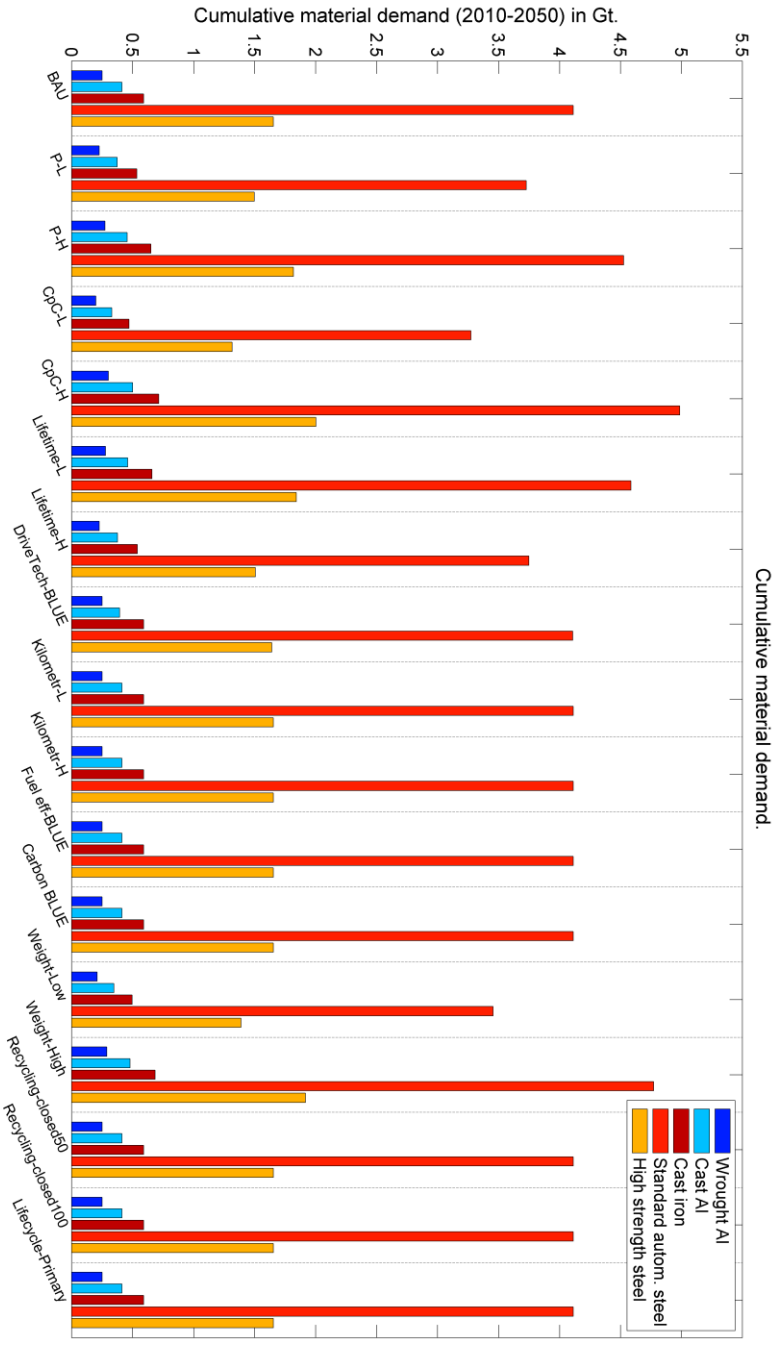

Figure S1-6: Cumulative material demand for the scenarios in the sensitivity analysis.

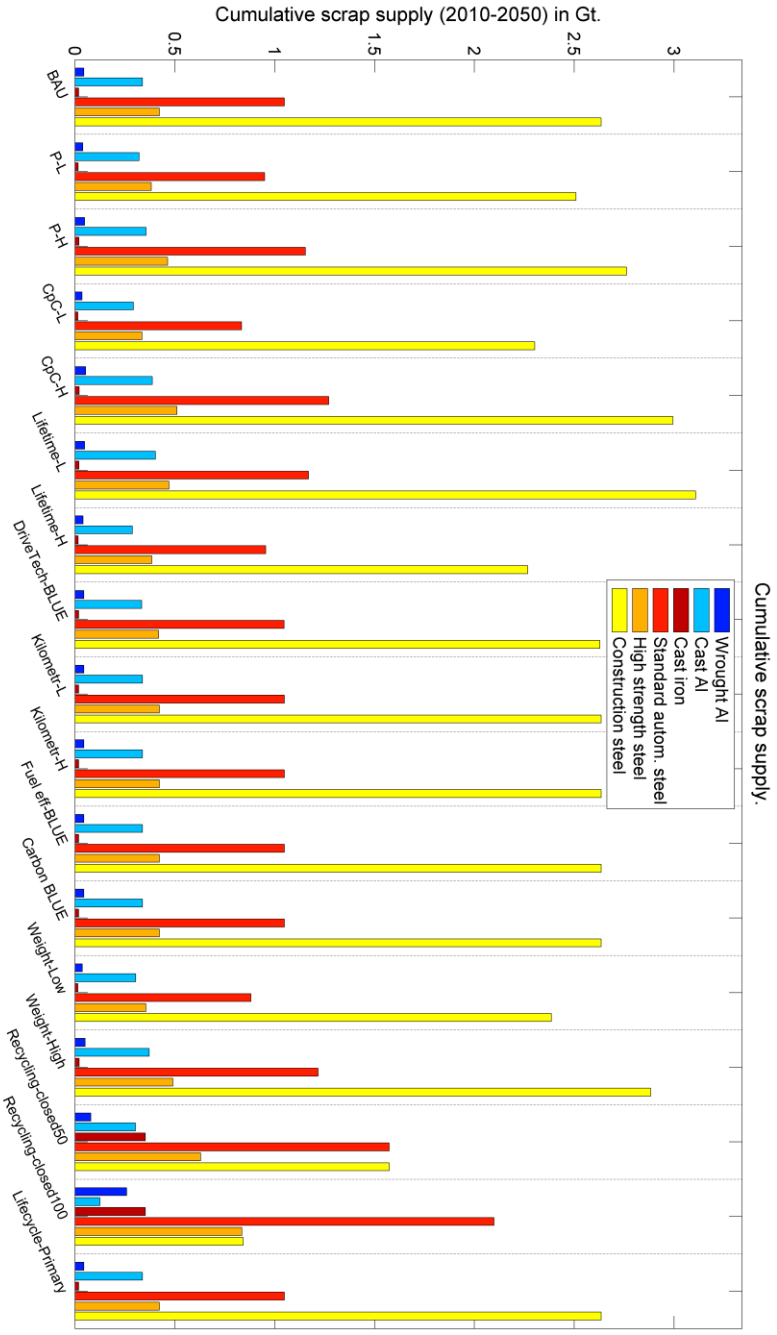

Figure S1-7: Cumulative supply of old scrap for the scenarios in the sensitivity analysis.

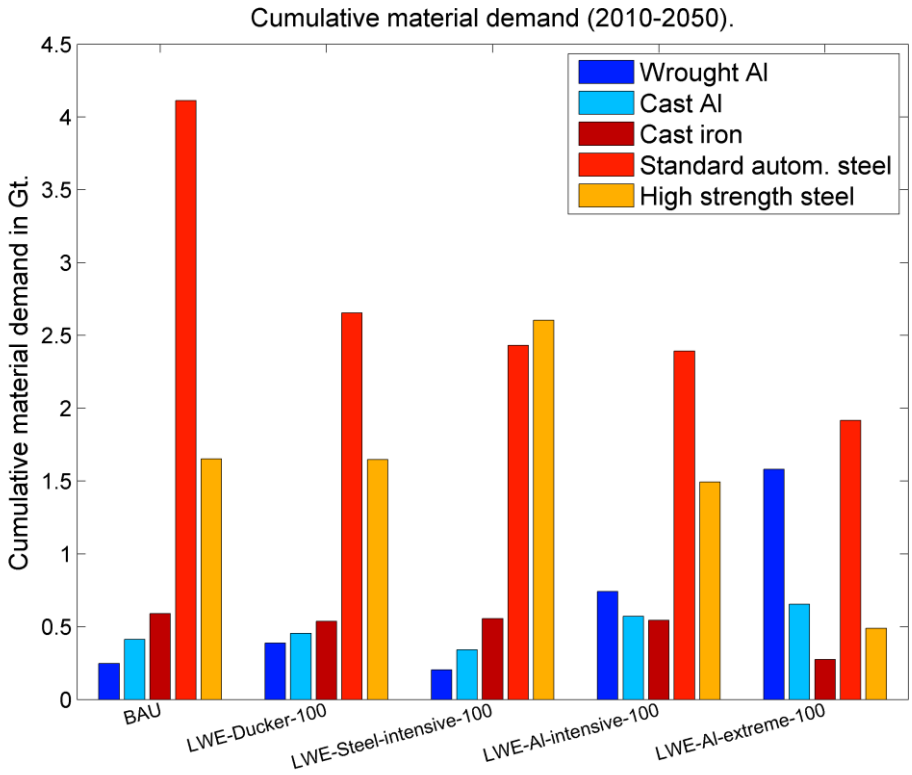

Figure S1-8: Cumulative material demand for the light-weighting scenarios.

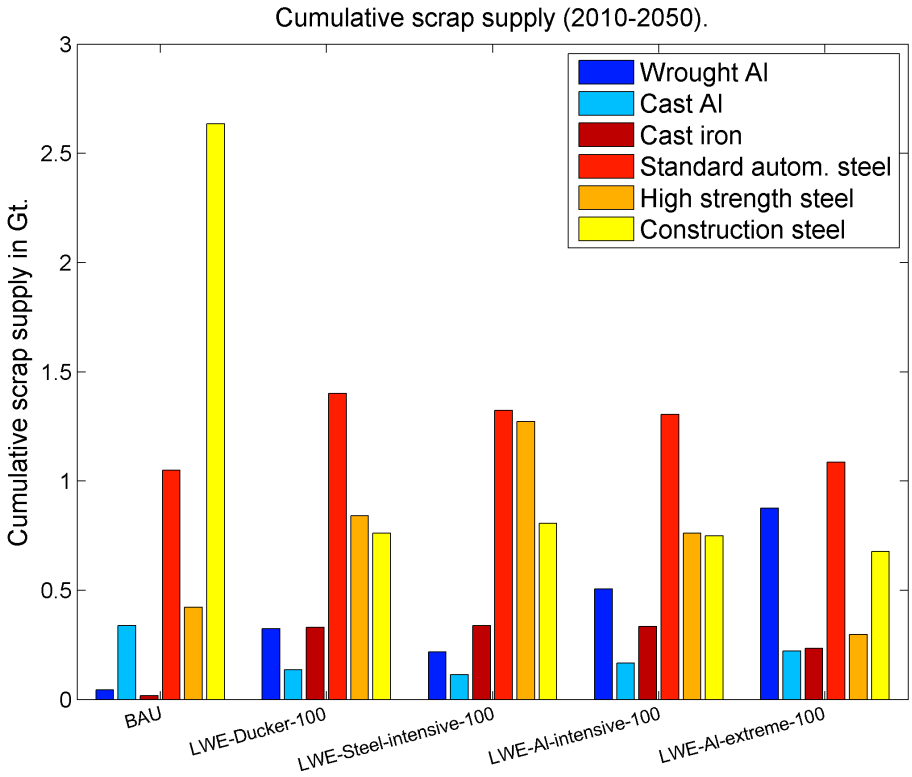

Figure S1-9: Cumulative supply of old scrap for the light-weighting scenarios.

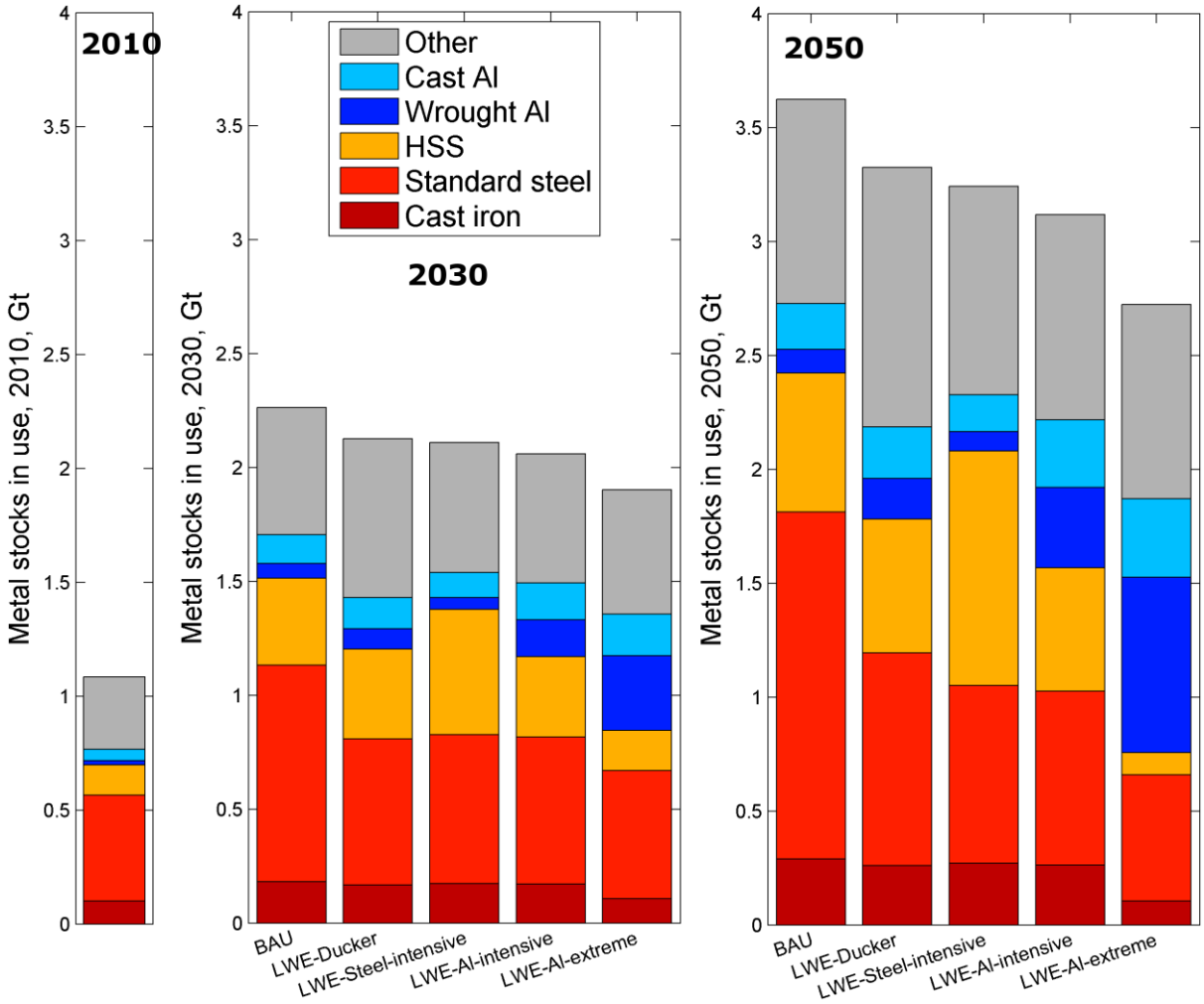

Figure S1-10: Stocks of materials contained in passenger cars in use for the global passenger vehicle fleet, 2010, 2030, and 2050. Divided by light-weighting scenario.

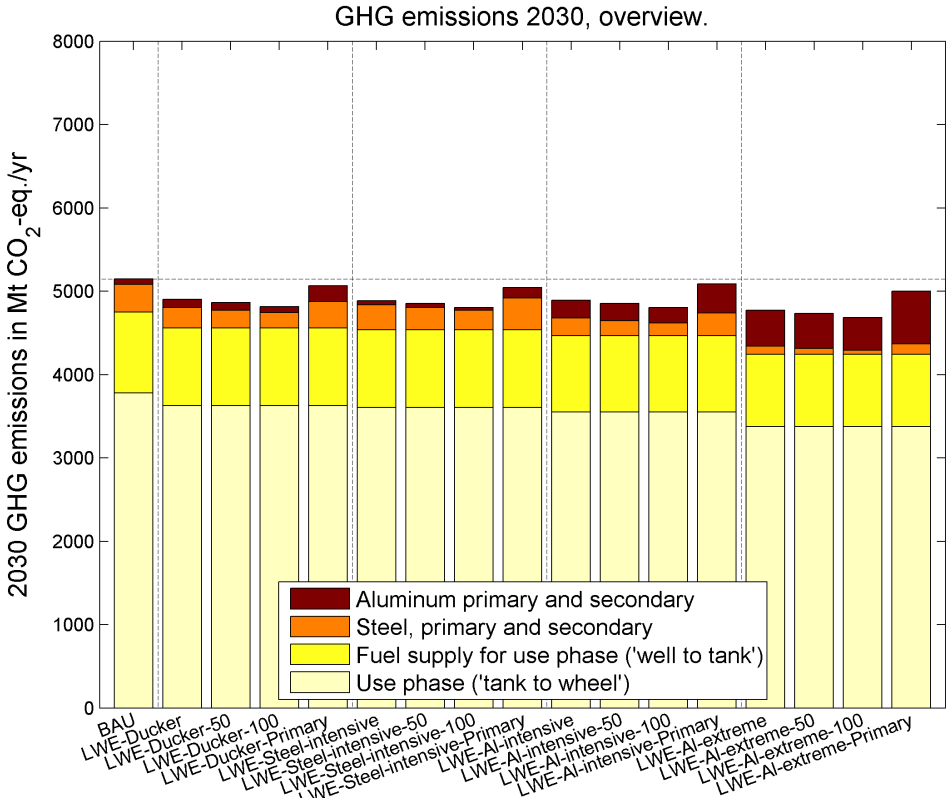

Figure S1-11: Annual carbon emissions from the use phase, fuel supply, and metal production, 2030.

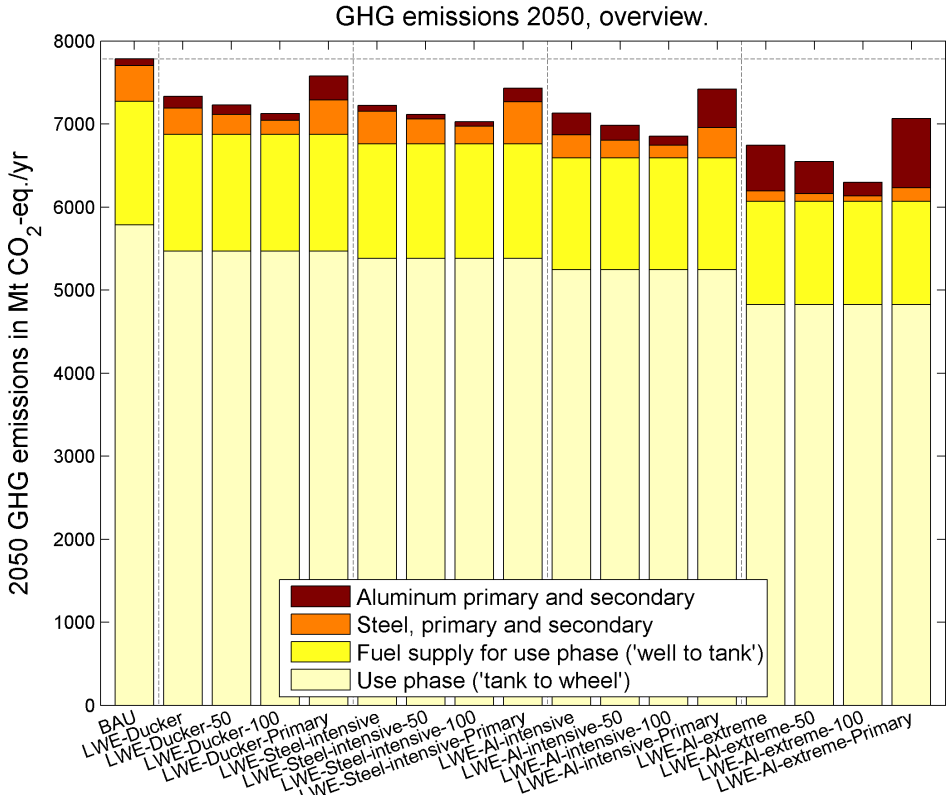

Figure S1-12: Annual carbon emissions from the use phase, fuel supply, and metal production, 2050.

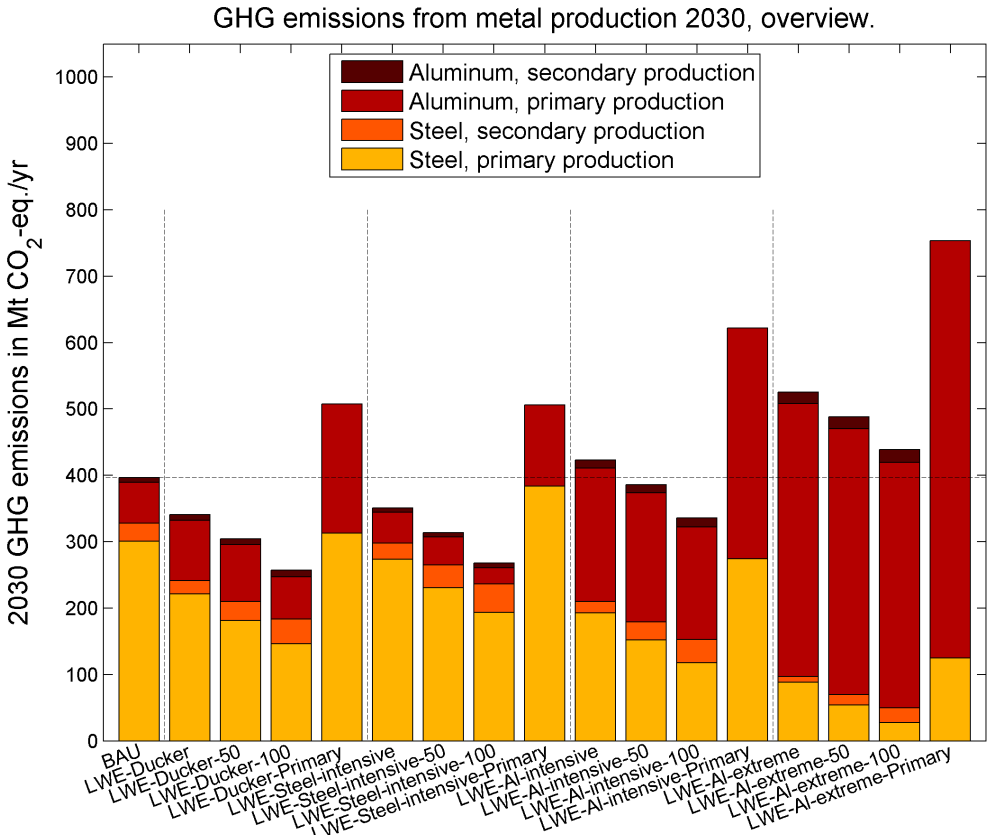

Figure S1-13: Annual carbon emissions from metal production, 2030.

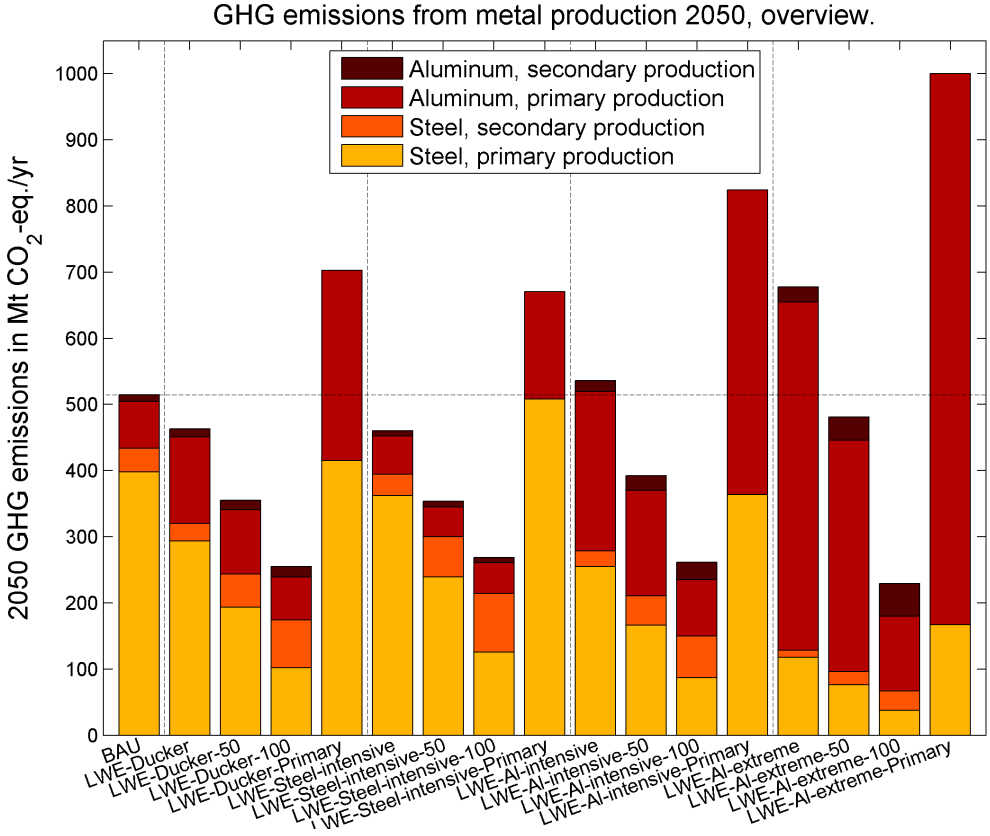

Figure S1-14: Annual carbon emissions from metal production, 2050.

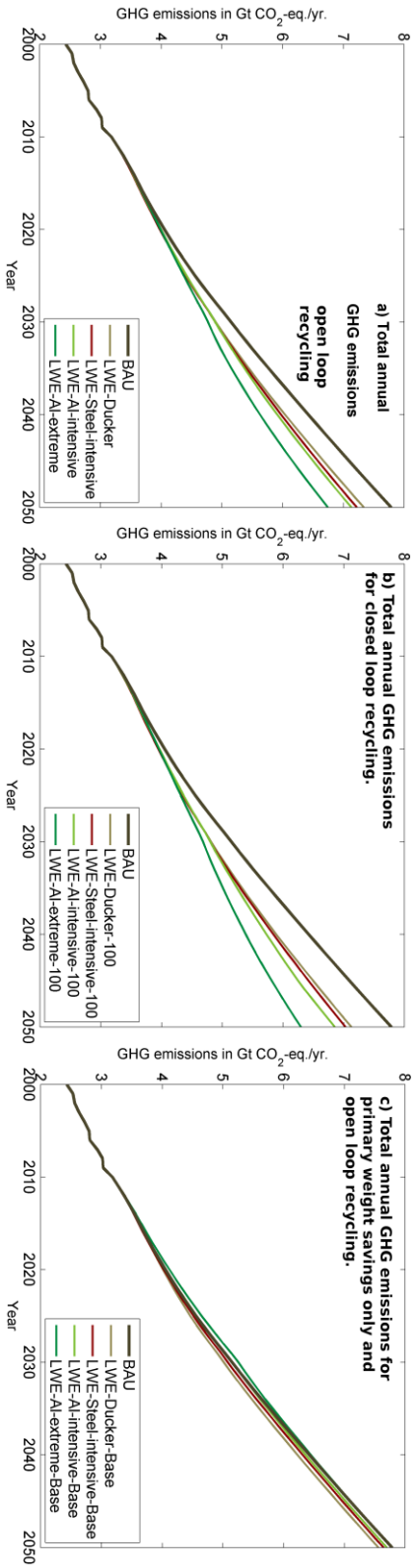

Figure S1-15: Total annual carbon emissions for the different light-weighting scenarios. **a)** Emissions by scenario, including secondary weight reductions and open loop recycling. **b)** Emissions by scenario, including secondary weight reductions and closed loop recycling. **c)** Emissions by scenario, including primary weight reductions and open loop recycling.

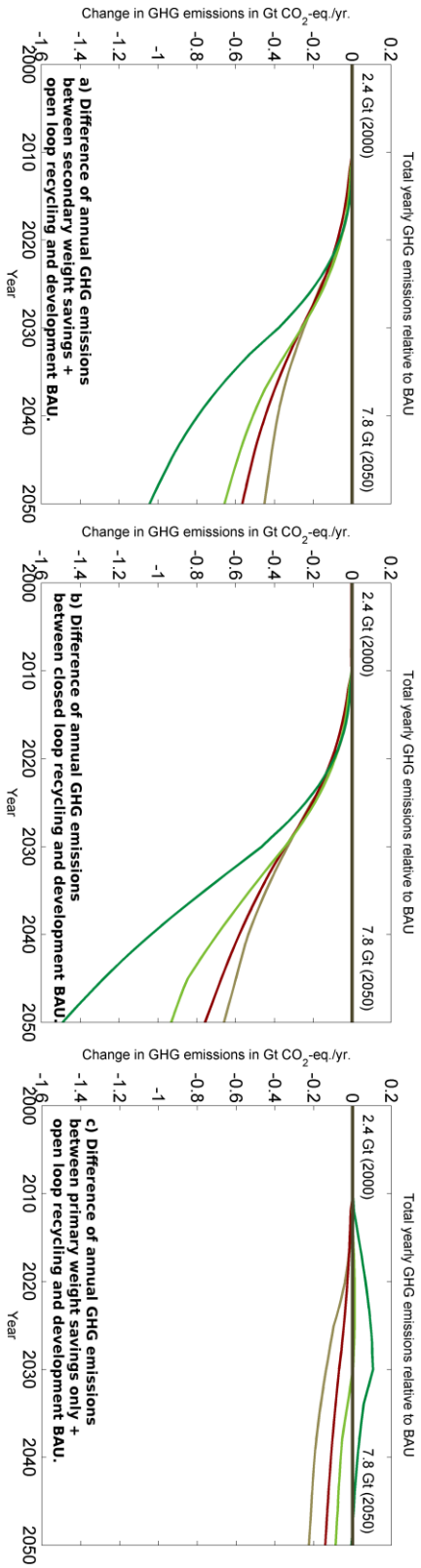

Figure S1-16: Annual carbon emissions for the different light-weighting scenarios, absolute difference compared to BAU scenario. **a)** Emissions by scenario, including secondary weight reductions and open loop recycling. **b)** Emissions by scenario, including secondary weight reductions and closed loop recycling. **c)** Emissions by scenario, including primary weight reductions and open loop recycling.

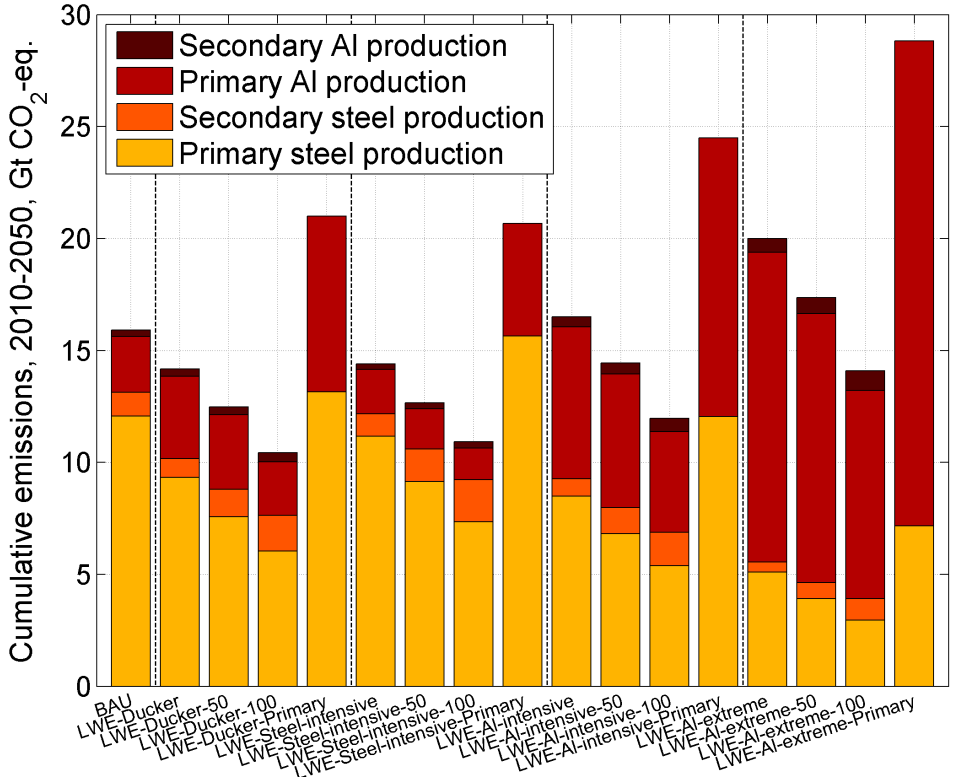

Figure S1-17: Cumulative GHG emissions for metal production and recycling, 2010-2050.

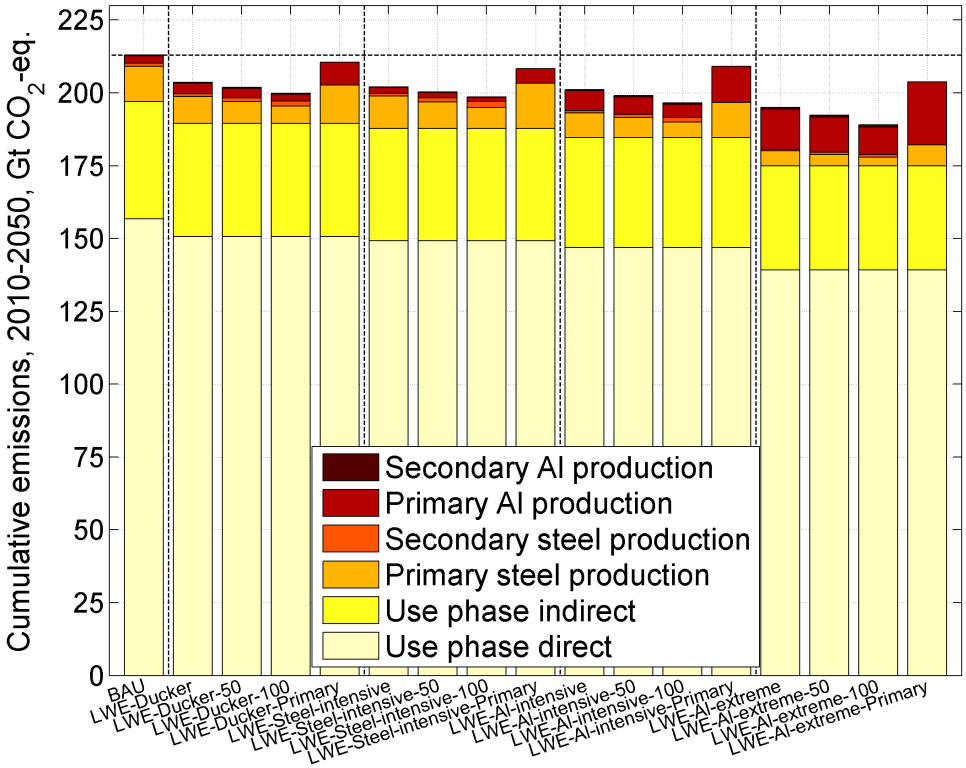

Figure S1-18: Cumulative GHG emissions for metal production, recycling, use, and fuel supply, 2010-2050.

S1-4) References

1. Müller, D. B., Stock dynamics for forecasting material flows-case study for housing in the Netherland. *Ecological Economics* **2006,** *59*, 152-156.
2. Modaresi, R.; Müller, D. B., The Role of Automobiles for the Future of Aluminum Recycling. *Environmental Science & Technology* **2012,** *46*, (16), 8587-8594.
3. Pauliuk, S.; Dhaniati, N. M. A.; Müller, D. B., Reconciling Sectoral Abatement Strategies with Global Climate Targets: The Case of the Chinese Passenger Vehicle Fleet. *Environ. Sci. Technol.* **2012,** *46*, (1), 7.
4. UN, World Population Prospects: The 2012 Revision **2014**.
5. Mitchell, B. R., *International historical statistics: Africa, Asia & Oceania, 1750-2005*. Palgrave Macmillan: Houndmills, 2007; p XXVII, 1175 s.
6. Mitchell, B. R., *International historical statistics: Europe 1750-2005*. Palgrave Macmillan: Houndmills, 2007; p XXI, 1068 s.
7. Mitchell, B. R., *International historical statistics: the Americas 1750-2005*. Palgrave Macmillan: Houndmills, 2007; p XIX, 875 s.
8. IEA *Energy Technology Perspectives, Scenarios Strategies to 2050* OECD/IEA: Paris, 2010.
9. Müller, D. B.; Cao, J.; Kongar, E.; Altonji, M.; Weiner, P.-H.; Graedel, a. T. E. *Service Lifetimes of Mineral End Uses*; U.S. Geological Survey (USGS),: 2007.
10. Kagawa, S.; Nansai, K.; Kondo, Y.; Hubacek, K.; Suh, S.; Minx, J.; Kudoh, Y.; Tasaki, T.; Nakamura, S., Role of Motor Vehicle Lifetime Extension in Climate Change Policy. *Environmental Science & Technology* **2011,** *45*, (4), 1184-1191.
11. Ducker Worldwide *Aluminum in 2012 North Americal Light Vehicles - executive summary*; 2011.
12. Ducker Worldwide *EAA Aluminium penetration in cars, Final Report, public version*; 2012.
13. Lutsey, N. *Review of technical literature and trends related to automobile mass-reduction technology*; California Air Resources Board: 2010.
14. America Iron and Steel Institute; Ducker Worldwide Light vehicle steel content - executive summary. http://www.autosteel.org/~/media/Files/Autosteel/Research/AHSS/Ducker%20Survey%20Results%20-%20AHSS%20Growth.pdf (May 23, 2014),
15. Hawkins, T. R.; Singh, B.; Majeau-Bettez, G.; Stromman, A. H., Comparative Environmental Life Cycle Assessment of Conventional and Electric Vehicles. *Journal of Industrial Ecology* **2013,** *17*, (1), 53-64.
16. EAA *Environmental Profile Report for the European Aluminium Industry*; European Aluminium Association (EAA): 2008.
17. Ducker, Aluminum in 2012 North American Light Vehicles. **2011**.
18. Pinto, A. S. A. F. Evolution of weight, fuel consumption and CO2 of automobiles. Universidade Tecnica de Lisboa, Instituto Superior Tecnico, 2009.
19. Ward's-Automotive, Ward's Motor Vehicle Facts and Figures, Material use in a typical family vehicle. In 2006.
20. Ducker Worldwide Aluminum in 2012 North Americal Light Vehicles - executive summary. http://www.autosteel.org/~/media/Files/Autosteel/Research/AHSS/Ducker%20Survey%20Results%20-%20AHSS%20Growth.pdf (May 23, 2014),
21. Ruifrok, R.; Vloemans, R.; Prinsen, S.; Waaijer, A., Best of Both Metals in Body Parts Light Weight Concepts for a Hood. *SAE Tech. Pap. Ser.* **1999,** *1999-01-3197*.
22. Marklund, P.-O.; Nilsson, L.; Rahmn, S.; Jonsson, M.; Svantesson, T.; Hellgren, L.-O., Optimization of a Press Hardened B-pillar by Use of the Response Surface Method. *SAE Tech. Pap. Ser.* **1999,** *1999-01-3236*.
23. van Schaik, M., Advanced High-Strength Steels and Hydroforming Reduce Mass and Improve Dent Resistance of Light Weight Doors In UltraLight Steel Auto Closures Project. *SAE Tech. Pap. Ser.* **2001,** *2001-01-3116*.
24. Shaw, J.; Engl, B.; Espina, C.; Oren, E. C.; Kawamoto, Y., ULSAB-Advanced Vehicle Concepts - Materials. *SAE Tech. Pap. Ser.* **2002,** *2002-01-0044*.
25. Cazes, C.; Ronin, F., Use of HSS1, VHSS2 and UHSS3 Steels in the Body in White: A Panorama of the Latest European Vehicles, State of Art and Perspectives. *SAE Tech. Pap. Ser.* **2002,** *2002-01-2049*.

26. Cazes, C.; Guillermin, L.; Duroux, P., Innovative Steel Solution for Body-in-White Parts. *SAE Tech. Pap. Ser.* **2003,** *2003-01-2846*.
27. McGuire, J. P., Materials Selection for Automotive Closure Applications with Respect to Cost and Function. *SAE Tech. Pap. Ser.* **2003,** *2003-01-2885*.
28. Sohmshetty, R.; Mallela, K., Advanced High Strength Steels for Chassis Structures. *SAE Tech. Pap. Ser.* **2008,** *2008-01-0854*.
29. Mallen, R. Z.; Odell, J.; O'Hara, B., Development of a 980MPa Center Pillar Structure for an SUV. *SAE Tech. Pap. Ser.* **2009,** *2009-01-0088*.
30. Laxman, S.; Iyengar, R. M.; Morgans, S., Achieving Light-Weight Design of Automotive Bodies with Advanced High Strength Steels via Structural Optimization. *SAE Tech. Pap. Ser.* **2009,** *2009-01-0795*.
31. Codd, D. S., Automotive Mass Reduction with Martensitic Stainless Steel. *SAE Tech. Pap. Ser.* **2011,** *2011-01-0427*.
32. Faath, T.; McKune, P.; Weber, M., InCar - Advanced High Strength Steel Tailored Tube Longitudinal Members. *SAE Tech. Pap. Ser.* **2011,** *2011-01-1061*.
33. Bhagwan, A.; McKune, P.; Faath, T.; Knoerr, L., InCar - Advanced Door Design. *SAE Int. J. Mater. Manf.* **2012,** *5*, (1), 235-246.
34. Fitz, F.; Gadd, C., Development of a Light Weight Passenger Car Wheel Using Conventional Steels and Fabrication Techniques. *SAE Tech. Pap. Ser.* **1999,** *1999-01-0782*.
35. van Schaik, M., ULSAB - Advanced Vehicle Concepts - Chassis and Suspension. In SAE International: 2002.
36. Chen, G.; Konieczny, A. A., Influence of AHSS Part Geometric Features on Crash Behavior. *SAE Tech. Pap. Ser.* **2006,** *2006-01-1588*.
37. Fuchs, H.; Salmon, R., Lightweight MacPherson Strut Suspension Front Lower Control Arm Design Development. *SAE Tech. Pap. Ser.* **2011,** *2011-01-0562*.
38. Vangipuram, R., Failure Mode Characterization of AHSS in Automotive Seat Structure Assemblies. *SAE Tech. Pap. Ser.* **2007,** *2007-01-0791*.
39. European Aluminium Association The Aluminium Automotive Manual - Applications - Car body - Body structures. http://www.alueurope.eu/wp-content/uploads/2011/12/1_AAM_Body-structures.pdf (May 23, 2014),
40. European Aluminium Association The Aluminium Automotive Manual - Applications - Car body - Body components. http://www.alueurope.eu/wp-content/uploads/2011/12/2_AAM_Body-Components.pdf (May 23, 2014),
41. European Aluminium Association The Aluminium Automotive Manual - Applications - Car body - Crash management systems. http://www.alueurope.eu/wp-content/uploads/2011/12/4_AAM_Crash-management-systems1.pdf (May 23, 2014),
42. European Aluminium Association The Aluminium Automotive Manual - Applications - Car body - Interior and other applications. http://www.alueurope.eu/wp-content/uploads/2011/12/7_AAM_Interior-and-other-applications.pdf (May 23, 2014),
43. European Aluminium Association The Aluminium Automotive Manual - Applications - Chassis & Suspension - Subframes. http://www.alueurope.eu/wp-content/uploads/2011/11/AAM-Applications-Chassis-Suspension-1-Subframes.pdf (May 23, 2014),
44. European Aluminium Association The Aluminium Automotive Manual - Applications - Chassis & Suspension - Suspension parts. http://www.alueurope.eu/wp-content/uploads/2011/11/AAM-Applications-Chassis-Suspension-2-Suspension-parts.pdf (May 23, 2014),
45. European Aluminium Association The Aluminium Automotive Manual - Applications - Chassis & Suspension - Wheels. http://www.alueurope.eu/wp-content/uploads/2011/11/AAM-Applications-Chassis-Suspension-3-Wheels.pdf (May 23, 2014),
46. European Aluminium Association The Aluminium Automotive Manual - Applications - Power train - Engine blocks. http://www.alueurope.eu/wp-content/uploads/2011/11/AAM-Applications-Power-train-2-Engine-blocks.pdf (May 23, 2014),
47. Alonso, E.; Lee, T. M.; Bjelkengren, C.; Roth, R.; Kirchain, R. E., Evaluating the Potential for Secondary Mass Savings in Vehicle Light-weighting. *Environ Sci Technol* **2012,** *46*, (5), 2893-2901.
48. Savov, L. V. E. J. D., Copper and tin in steel scrap recycling = baker in kositer v recikliranem starem zelezu. *RMZ - Materials and geoenvironment* **2003,** *50*, (3), 627-641.
49. Bajželj, B.; Allwood, J. M.; Cullen, J. M., Designing Climate Change Mitigation Plans That Add Up. *Environmental Science & Technology* **2013,** *47*, (14), 8062-8069.

50. Pauliuk, S.; Milford, R. L.; Müller, D. B.; Allwood, J. M., The Steel Scrap Age. *Environmental Science & Technology* **2013,** *47*, (7), 3448-3454.
51. WorldSteel, The three Rs of sustainable steel. In World Steel Association: 2010.
52. Liu, G.; Bangs, C.; Müller, D. B., Stock dynamics and emission pathwaysof the global aluminium cycle. *Nature Climate Change,* **2012**.
53. Cullen, J. M.; Allwood, J. M., Mapping the Global Flow of Aluminum: From Liquid Aluminum to End-Use Goods. *Environmental Science & Technology* **2013,** *47*, (7), 3057-3064.
54. Cullen, J. M.; Allwood, J. M.; Bambach, M. D., Mapping the Global Flow of Steel: From Steelmaking to End-Use Goods. *Environmental Science & Technology* **2012,** *46*, (24), 13048-13055.
55. Cheah, L. W. Cars on a Diet: The Material and Energy Impacts of Passenger Vehicle Weight Reduction in the U.S. MIT, 2010.
56. Martin Johannaber, M. E., Roland Wohlecker, Henning Wallentowitz, Jörg Leyers *Determination of Weight Elasticity of Fuel Economy for Conventional ICE Vehicles, Hybrid Vehicles and Fuel Cell Vehicles*; Forschungsgesellschaft Kraftfahrwesen mbH Aachen (FKA): Aachen, 2007.
57. Kim, H. C.; Wallington, T. J., Life-Cycle Energy and Greenhouse Gas Emission Benefits of Light-weighting in Automobiles: Review and Harmonization. *Environmental Science & Technology* **2013,** *47*, (12), 6089-6097.
58. Milford, R. L.; Pauliuk, S.; Allwood, J. M.; Müller, D. B., The Roles of Energy and Material Efficiency in Meeting Steel Industry CO2 Targets. *Environmental Science & Technology* **2013,** *47*, (7), 3455-3462.
59. Worrell, E.; Bernstein, L.; Roy, J.; Price, L.; Harnisch, J., Industrial energy efficiency and climate change mitigation. *Energy Efficiency* **2009,** *2*, (2), 109-123.
60. Kim, H.-J.; McMillan, C.; Keoleian, G. A.; Skerlos, S. J., Greenhouse Gas Emissions Payback for Lightweighted Vehicles Using Aluminum and High-Strength Steel. *Journal of Industrial Ecology* **2010,** *14*, (6).
61. IAI *Global Aluminium Recycling: A Cornerstone of Sustainable Development*; International Aluminium Institute: 2009.
62. GARC, GARC model. In 2007.
63. Liu, G.; Bangs, C. E.; Muller, D. B., Stock dynamics and emission pathways of the global aluminium cycle. *Nature Clim. Change* **2013,** *3*, (4), 338-342.
64. Bioenergy Conversion Factor. https://bioenergy.ornl.gov/papers/misc/energy_conv.html (2013-10-12),
65. *CO2 Emissions from Fuel Combustion - Highlights*; IEA: Paris, France, 2012.
66. Pont, J. *Full Fuel Cycle Assessment- Well to Tank Energy Inputs, Emissions, And Water Impacts*; TIAX, LLC: CA, USA, 2007.